Journal of Computational Neuroscience, 36(1): 97–118, 2014.

A single functional model of drivers and modulators in cortex

M. W. Spratling
King's College London, Department of Informatics, London. UK.

Abstract

A distinction is commonly made between synaptic connections capable of evoking a response ("drivers") and those that can alter ongoing activity but not initiate it ("modulators"). Here it is proposed that, in cortex, both drivers and modulators are an emergent property of the perceptual inference performed by cortical circuits. Hence, it is proposed that there is a single underlying computational explanation for both forms of synaptic connection. This idea is illustrated using a predictive coding model of cortical perceptual inference. In this model all synaptic inputs are treated identically. However, functionally, certain synaptic inputs drive neural responses while others have a modulatory influence. This model is shown to account for driving and modulatory influences in bottom-up, lateral, and top-down pathways, and is used to simulate a wide range of neurophysiological phenomena including surround suppression, contour integration, gain modulation, spatio-temporal prediction, and attention. The proposed computational model thus provides a single functional explanation for drivers and modulators and a unified account of a diverse range of neurophysiological data.

Keywords: cerebral cortex; cortical feedback; lateral connections; gain modulation; surround suppression; attention

1 Introduction

Neural response modulation occurs when a stimulus, which causes little or no response when presented in isolation, has a significant effect on the the firing rate of a neuron in response to another stimulus. Such modulatory interactions are a common feature of neuronal activity having been observed in many different regions of the brain and in association with many different cognitive functions. For example, the modulation of visually-driven responses by gaze direction, head orientation or hand posture that is thought to underlie spatial reference frame remapping (Andersen et al., 1985; Andersen and Mountcastle, 1983; Bremmer et al., 1997; Brotchie et al., 1995; Chang and Snyder, 2010; Galletti et al., 1995), the modulation of sensory-driven responses by attentional state or prior expectation (Chelazzi et al., 2001; Kastner and Ungerleider, 2000; Martinez-Trujillo and Treue, 2004; McAdams and Maunsell, 1999a; Reynolds et al., 1999), and the modulatory effects of visual stimuli presented to the non-classical receptive field (ncRF) of cells in primary visual cortex (V1) (Angelucci and Bullier, 2003; Jones et al., 2001; Kapadia et al., 2000; Seriès et al., 2003).

This has lead to a general distinction being made between driving and modulatory influences (Crick and Koch, 1998; Pasquale and Sherman, 2011; Sherman and Guillery, 1998), and to modulatory effects being proposed as a common computational mechanism employed throughout the cerebral cortex (Kay and Phillips, 2011; Phillips and Singer, 1997; Salinas and Sejnowski, 2001; Salinas and Thier, 2000). Here an alternative functional explanation for drivers and modulators is proposed: that both drivers and modulators result from the cortex performing perceptual inference. This idea is illustrated using the predictive coding/biased competition (PC/BC) model of cortical function (Spratling, 2008a,b).

PC/BC is a hierarchical neural network model. In each stage of this hierarchy, neurons represent predictions of the causes underlying the inputs to that stage. These predictions are updated by comparing the inputs reconstructed from these predictions with the actual inputs and using the resulting error to modify the predictions so as to minimise the reconstruction error. This ongoing, iterative, process results in the predictions being continuously updated to find those that best explain the inputs. Some inputs provide unambiguous evidence for certain predictions, and hence, drive responses from the neurons that represent those predictions. Other inputs can produce both facilitatory and suppressive modulatory influences. Facilitatory modulation results from inputs that are ambiguous. These inputs provide weak evidence to support many alternative predictions, and hence, have little influence on prediction neuron responses when presented in isolation. However, when presented simultaneously with driving inputs, these ambiguous inputs add to the evidence supporting one prediction, and hence, strongly increase the response of the neuron that represents that prediction. Suppressive modulation results from inputs that drive alternative, competing, interpretations of the input. When such inputs provide strong evidence for a second explanation of the input, the evidence for the first prediction can be "explained away" (Kersten et al., 2004; Lochmann and Deneve, 2011) leading to strong suppression of the response of the neuron that represents the first prediction.

In the proposed model, whether a synaptic connection is modulatory or driving depends on its role in the inference process: its influence is dependent on the evidence that it provides to support different hypotheses. In the proposed model, a synaptic connection's influence is *not* dependent on its anatomical source of origin. Indeed, inter-cortical feedforward and feedback connections, long-range intra-cortical lateral connections, and thalamic inputs, are all treated identically by the model, and a PC/BC processing stage does not know the source of origin of the inputs it receives. This means that in the proposed model feedback connections, just like feedforward connections, can contain both driving synapses and modulatory synapses. In contrast previous theories of cortical function have proposed that cortical feedback connections have properties that are distinct from those of feedforward connections. Specifically, many previous theories (including most versions of biased competition) propose that cortical feedback is *modulatory* while feedforward connections are driving (*e.g.*, Crick and Koch, 1998; Friston, 2009; Friston and Büchel, 2000; Hupé et al., 1998; Koch and Segev, 2000; Kveraga et al., 2007; Lamme et al., 1998; Olshausen et al., 1993; Reynolds et al., 1999; Reynolds and Desimone, 1999). A rival set of theories (including most versions of predicitive coding) propose that cortical feedback is *inhibitory* while feedforward connections are driving (*e.g.*, Barlow, 1994; Friston, 2005; Koerner et al., 1997; Mumford, 1992; Rao and Ballard, 1999). Unlike the proposed model, these previous theories are in conflict with empirical evidence that cortical feedback connections can have both modulatory and driving influences. Physiological evidence that feedback can have a driving influences is reviewed in Markov and Kennedy (2013) and Muckli and Petro (2013), while physiological evidence that feedback can have a modulatory influence comes from numerous experiments on attention (*e.g.*, Kanwisher and Wojciulik, 2000; Kastner et al., 1999; Luck et al., 1997; McAdams and Maunsell, 2000; Treue, 2001) which is typically believed to operate via the cortical feedback projections (Buffalo et al., 2010; Desimone and Duncan, 1995; Mehta et al., 2000b; Pollen, 1999; Schroeder et al., 2001; Treue, 2001). Recent anatomical evidence also suggests that cortical feedback connections contain both modulatory and driving synapses (Covic and Sherman, 2011; Pasquale and Sherman, 2011). Hence, while PC/BC is closely related to both predictive coding and biased competition (De Meyer and Spratling, 2011; Spratling, 2008a), it is more consistent than either of these theories with the known properties of cortical feedback pathways.

2 Methods

2.1 PC/BC with Feedforward Connections

The main mathematical operation required to implement the PC/BC algorithm is the calculation of sums of products. The algorithm can therefore be implemented, equally simply, using matrix multiplication or linear filtering operations. The latter implementation method is particularly useful for image processing as neurons with the same RFs are replicated at every pixel location. The results presented in this article have been generated using both the matrix implementation of PC/BC and the filtering implementation. Hence, both implementations will be described in the following paragraphs.

PC/BC using matrix multiplication is illustrated in Fig. 1a and implemented using the following equations:

$$\mathbf{e} = \mathsf{G}\left(\mathbf{x}\right) \oslash \left(\epsilon_2 + \mathbf{V}^T\mathbf{y}\right) \tag{1}$$

$$\mathbf{y} \leftarrow \left(\epsilon_1 + \mathbf{y}\right) \otimes \mathbf{We} \tag{2}$$

Where $\mathbf{e}$ is a (m by 1) vector of error-detecting neuron activations; $\mathbf{y}$ is a (n by 1) vector of prediction neuron activations; $\mathbf{W}$ is a (n by m) matrix of feedforward synaptic weight values; $\mathbf{V}$ is a (n by m) matrix of feedback synaptic weight values; ϵ_1 and ϵ_2 are parameters; $\oslash$ and $\otimes$ indicate element-wise division and multiplication respectively (addition operations are also performed element-wise); and G is a function that clips values at 1 (*i.e.*, $\mathsf{G}(x) = x\ \forall x \leq 1; \mathsf{G}(x) = 1\ \forall x > 1$). This is used to prevent runaway increases in prediction neuron responses caused by positive feedback effects in reciprocally connected networks (see below). Each row of $\mathbf{W}$ represents the synaptic weights of an individual prediction neuron. Typically, the rows of $\mathbf{W}$ are normalised to sum to one. $\mathbf{V}$ is equal to $\mathbf{W}$ except that the rows of $\mathbf{V}$ are normalised to have a maximum value of one. Hence, the feedforward and feedback weights are simply rescaled versions of each other. How the weights are defined in order to simulate each experiment is described in subsequent sections.

Initially the values of $\mathbf{y}$ are all set to zero, although random initialisation of the prediction neuron activations can also be used with little influence on the results. Equations 1 and 2 are then updated for a number of iterations with the new values of $\mathbf{y}$ calculated by equation 2 substituted into equations 1 and 2 to recursively calculate the changing neural activations at each iteration. Parameter values of $\epsilon_1 = 1 \times 10^{-5}$ and $\epsilon_2 = 1 \times 10^{-3}$ were used in all the experiments reported in this article.

The values of $\mathbf{y}$ represent predictions of the causes underlying the inputs to the PC/BC network. The values of $\mathbf{e}$ represent the residual error between the input reconstructed from these predictions and the actual input, $\mathbf{x}$, to the

Figure 1: (a) The PC/BC neural network architecture implemented using matrix multiplication. White rectangles represent populations of neurons and arrows represent connections between populations of neurons. White arrow heads signify excitatory connections, black arrow heads indicate inhibitory connections. Black connections signify a many-to-many connectivity pattern between the neurons in two populations, and gray connections indicate a one-to-one mapping of connections between the neurons in two populations. Connection weights are represented by matrices: $\mathbf{W}$ for the feedforward weights, and $\mathbf{V}$ for the feedback weights. Neural responses are represented by vectors: $\mathbf{x}$ for the input stimulus, $\mathbf{e}$ for the error-detecting neurons, and $\mathbf{y}$ for the prediction neurons. (b) The PC/BC neural network architecture implemented using filtering. Each population of neurons may be represented by multiple sub-populations, or channels, describing the neural responses of a particular type, or class, of neuron in that population. White rectangles represent sub-populations of neurons. Neural responses in each sub-population are represented by a 2-dimensional array, or image: $\mathbf{X}_i$ for the input stimulus, $\mathbf{E}_i$ for the error-detecting neurons, and $\mathbf{Y}_j$ for the prediction neurons. Arrows represent connections between populations of neurons. White arrow heads signify excitatory connections, black arrow heads indicate inhibitory connections. Connection weights are represented by filters: $\mathbf{w}_{ji}$ for the feedforward weights, and $\mathbf{v}_{ji}$ for the feedback weights. Black connections signify a many-to-many connectivity pattern between sub-populations of neurons as well as a many-to-many connectivity pattern between the neurons in those sub-populations. Gray connections indicate a one-to-one mapping between sub-populations of neurons as well as a one-to-one mapping of connections between the neurons in those sub-populations.

network. Equation 2 describes the updating of the prediction neuron activations. The response of each prediction neuron is a function of its activation at the previous iteration and a weighted sum of afferent inputs from the error-detecting neurons. Equation 1 describes the calculation of the neural activity of the error-detecting neurons. These values are a function of the activity of the input to PC/BC divisively modulated by a weighted sum of the prediction neurons responses. The iterative process described above changes the values of $\mathbf{y}$ so as to minimise the error between actual inputs and the predicted inputs. This is achieved because if an element of $\mathbf{e}$ is greater than one (respectively less than one) prediction neurons that receive input from that error-detecting neuron will increase (decrease) their response (via equation 2). The output of the prediction neurons will then more strongly (weakly) represent the predicted causes of the input, which will in turn reduce (increase) the residual error encoded by that element of $\mathbf{e}$ (via equation 1).

PC/BC using filtering is illustrated in Fig. 1b and implemented using the following equations:

$$\mathbf{E}_i = \mathsf{G}\left(\mathbf{X}_i\right) \oslash \left(\epsilon_2 + \sum_{j=1}^{p} \left(\mathbf{v}_{ji} * \mathbf{Y}_j\right)\right) \tag{3}$$

$$\mathbf{Y}_j \leftarrow \left(\epsilon_1 + \mathbf{Y}_j\right) \otimes \left(\sum_{i=1}^{k} \left(\mathbf{w}_{ji} \star \mathbf{E}_i\right)\right) \tag{4}$$

Where $\mathbf{X}_i$ is a 2-dimensional input image; $\mathbf{E}_i$ is a 2-dimensional array, equal in size to the input image, that represents the error-detecting neuron responses; $\mathbf{Y}_j$ is a 2-dimensional array, equal in size to the input image, that represent the prediction neuron responses for a particular class, j, of prediction neuron; $\mathbf{w}_{ji}$ is a 2-dimensional kernel representing the feedforward synaptic weights from a particular channel, i, of the input to a particular class, j, of prediction neuron; $\mathbf{v}_{ji}$ is a 2-dimensional kernel representing the feedback synaptic weights from a particular class, j, of prediction neuron to a particular channel, i of the input; ϵ_1 and ϵ_2 are parameters; $\oslash$ and $\otimes$ indicate element-wise division and multiplication respectively (addition operations are also performed element-wise); $\star$ represents cross-correlation (which is equivalent to convolution without the kernel being rotated 180^o); and $*$ represents convolution (which is equivalent to cross-correlation with a kernel rotated by 180^o). The application and behaviour of equations 3 and 4 is equivalent to the matrix version described above.

The feedforward weights to an individual prediction neuron are normalised to sum to one. The corresponding feedback weights are defined to be equal to the feedforward weights, except they are normalised to have a

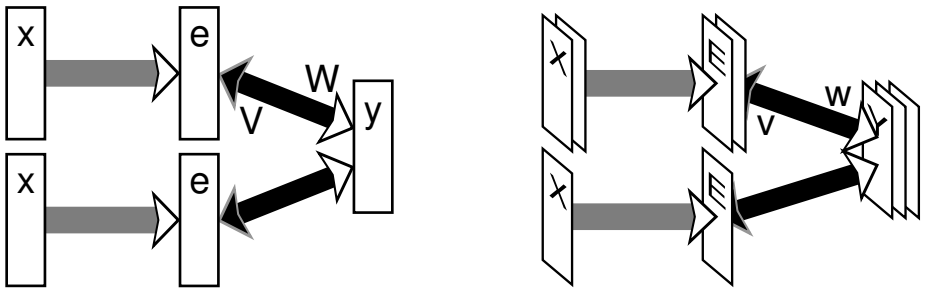

Figure 2: The PC/BC neural network architecture with multiple sources of input. (a) Implemented using matrix multiplication. The format of this diagram is identical to, and described in the caption of, Fig. 1a. (b) Implemented using filtering. The format of this diagram is identical to, and described in the caption of, Fig. 1b.

maximum value of one. Convolution is used in equation 3 while cross-correlation is used in equation 4 to ensure that the feedback weights between a prediction neuron and an error-detecting neuron correspond to the feedforward weights between the same two neurons, *i.e.*, this arrangement results in the feedforward weight between two neurons being identical to the feedback weight between the same two neurons (up to the different scaling applied to $\mathbf{w}_{ji}$ and $\mathbf{v}_{ji}$). The cross-correlation and convolution operations effectively reproduce prediction neurons with identical RFs at every pixel location in the image. This allows very large scale neural networks to be created easily. For example, to process the 512 by 512 pixel images used in Fig. 9 the PC/BC network contains approximately 8.4 million prediction neurons each of which has approximately 29 thousand synaptic inputs.

The inputs to a PC/BC processing stage are simply non-negative numbers: a vector, $\mathbf{x}$, of non-negative values in the matrix implementation of the model, or one or more arrays, $\mathbf{X}_i$, of non-negative values in the filtering implementation. These values could be provided by the the outputs (the prediction neuron responses) of a previous PC/BC processing stage in a hierarchy, or might represent external inputs to the model. In some circumstances it might be convenient to represent the input as coming from multiple, separate, sources. For example, if the input is arriving from separate PC/BC processing stages at a lower level in a hierarchy, or if inputs are coming from multiple sensory modalities. This is illustrated, for two sources of input, in Fig. 2. Multiple sources of input can be dealt with without modification to the equations. For the matrix implementation of PC/BC the multiple input vectors can be concatenated into a single vector and additional columns of synaptic weights can be added to matrices $\mathbf{W}$ and $\mathbf{V}$. For the filtering implementation of PC/BC, the index i needs to range over the additional input channels, and additional filters $\mathbf{w}$ and $\mathbf{v}$ need to be defined. Recurrent connections, as described in section 2.2, can also act as sources of additional inputs to the PC/BC model, and these can also be dealt with without modification to the equations, as described above.

2.2 PC/BC with Lateral Connections

A method of implementing lateral excitatory connections in the PC/BC model is illustrated in Fig. 3a. This diagram shows lateral connections in a PC/BC model implemented using filtering; lateral connectivity in the matrix version of PC/BC would be implemented analogously. Recurrent connections are used to take the outputs of the prediction neurons and use them as additional inputs to the PC/BC model. For the matrix implementation of PC/BC this means that the vector $\mathbf{x}$ becomes a concatenation of the original inputs and the outputs, $\mathbf{y}$, calculated at the preceding iteration. Similarly, for PC/BC implemented using filtering, this means that each output "image" of prediction neuron responses, $\mathbf{Y}_j$, is used to provide a new input image.

Note that it is not necessary to employ separate neural populations to represent the recurrent inputs: connections from the prediction neurons could go directly to the error neurons, and the additional populations of inputs could be omitted from the diagram, as shown in Fig. 3b. Additional populations of inputs are simply used for implementational, and explanatory, convenience.

Additional synaptic weights need to be defined to allow the recurrent inputs to influence the prediction neuron responses. For the matrix implementation of PC/BC, the additional weights will form additional columns of matrices $\mathbf{W}$ and $\mathbf{V}$. For the filtering implementation of PC/BC, additional filters $\mathbf{w}$ and $\mathbf{v}$ need to be defined. In the latter case the cross-correlation and convolution operations in equations 3 and 4 effectively reproduce the same pattern of lateral connectivity between prediction neurons with equivalent RFs at all locations in the model. The exact form of the lateral weights will determine how the recurrent inputs affect the behaviour of the model.

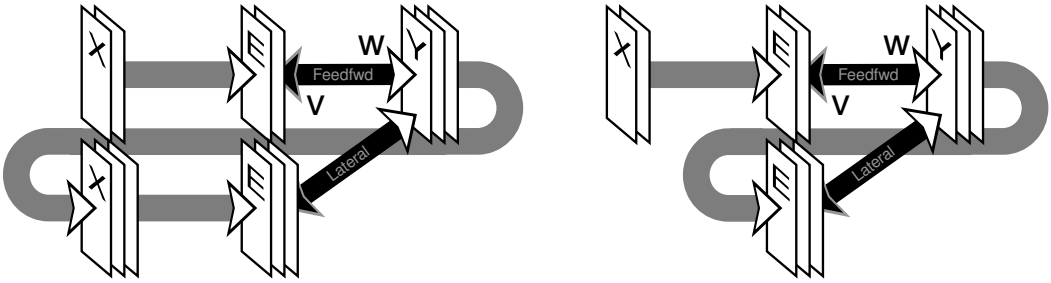

(a) (b)

Figure 3: The PC/BC neural network architecture with recurrent inputs providing lateral connectivity between the prediction neurons. Recurrent inputs shown (a) explicitly using a separate population of inputs, (b) without a separate population of inputs. The format of this diagram is identical to, and described in the caption of, Fig. 1b

2.3 PC/BC as a Model of Cortical Area V1

In several of the simulations reported in the Results, a processing stage in the PC/BC model is provided with synaptic weights to enable it to simulate the response properties of orientation selective neurons in primary visual cortex (V1). This model is implemented using the filtering method of implementing PC/BC. Brief details of this model of V1 are given in this section. Fuller details can be found in (Spratling, 2010). However, in contrast to this previous work, here RFs are defined as derivatives of Gaussians (rather than Gabors), and recurrent inputs are used to simulate long-range lateral connectivity in V1. Fuller implementation details for the pattern of lateral connectivity in the V1 model can be found in (Spratling, 2013).

To implement a model of primary visual cortex, the input to the PC/BC model is an input image (I) pre-processed by convolution with a Laplacian-of-Gaussian (LoG) filter (l) with standard deviation equal to σ_{LGN} pixels. The output from this filter is subject to a multiplicative gain (the strength of which was determined by parameter κ_{LGN}) followed by a saturating non-linearity, such that:

$$\mathbf{X} = \tanh\left(\kappa_{LGN}(I * l)\right)$$

Values of $\kappa_{LGN} = 2\pi$ and $\sigma_{LGN} = 2$ pixels were used in the simulations reported here. The positive and rectified negative responses are separated into two images $\mathbf{X}_{ON}$ and $\mathbf{X}_{OFF}$ simulating the outputs of cells in retina and LGN with circular-symmetric on-centre/off-surround and off-centre/on-surround RFs respectively. To avoid strong responses along the border of the input image, the $\mathbf{X}_{ON}$ and $\mathbf{X}_{OFF}$ values within a distance $3\sigma_{LGN}$ pixels from the border were set to zero.

The synaptic weights of the PC/BC model of V1 are defined as follows. $\mathbf{w}_{ji}$ and $\mathbf{v}_{ji}$ (where $i \in [ON, OFF]$), are defined using the first and second derivatives of a Gaussian. These functions were used as they closely match the pattern of response generated by the LoG filters (as used in the model of LGN) when applied to idealised step and ridge edges. The first and second derivatives of a Gaussian also resemble the RFs of a simple cells in primary visual cortex (Young and Lesperance, 2001). The weights used were the positive and negative of the second derivative of a Gaussian at orientations 0^o to 157.5^o in steps of 22.5^o, and the first derivative of a Gaussian at orientations 0^o to 337.5^o in steps of 22.5^o. Giving a family of 32 weight masks (*i.e.*, j ranged from 1 to 32). As the model is implemented using the filtering version of PC/BC, the same set of 32 weights are reproduced at every pixel location. Hence, prediction neurons with the same feature preferences (orientation and phase) are evenly distributed across the input image.

The Gaussian used to define the derivative of Gaussian filters had a length (the extent perpendicular to the axis along which the derivative was taken) defined by σ_{V1} and a width in the perpendicular direction defined by σ_{LGN}. The positive and rectified negative values of the Gaussian derivatives were separated and used to define the weights to the ON and OFF channels of the input. A value of $\sigma_{V1} = 3$ pixels was used in the simulations reported here.

In simulations where the V1 model included lateral connections, two sets of prediction neurons with identical feedforward RFs, but with different patterns of lateral weights were used. For each pair of prediction neurons with identical RFs, one neuron was used to respond to texture edges the other to boundary edges. Given that the RFs are the same, it is purely differences in the lateral connectivity that differentiates prediction neurons that operate as texture edge detectors from those that act as boundary edge detectors. This is similar to some models of cortical area V2 which employ neurons representing boundaries that come in pairs to represent different configurations of

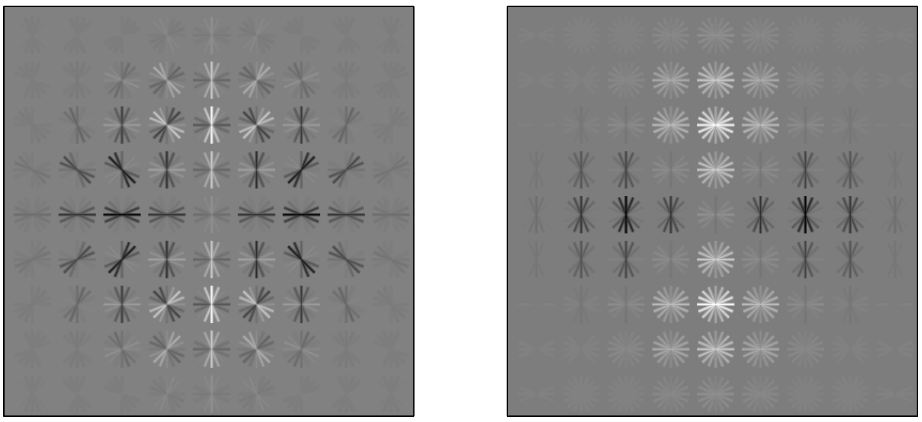

(a) (b)

Figure 4: Lateral connections. Each image shows the strength of the lateral connections received by a post-synaptic prediction neuron with a horizontally oriented RF at the centre of the image. Each line segment indicates the RF location and orientation of the pre-synaptic prediction neuron. The strength of each connection is indicated by the shading of the line segment: black indicates strong connections from prediction neurons representing boundary edges, white represents strong connections from prediction neurons representing texture edges. (a) shows the lateral connections received by a prediction neuron representing a horizontal boundary edge at the centre of the image, (b) shows the lateral connections received by a prediction neuron representing horizontal texture edge at the centre of the image.

border-ownership (Craft et al., 2007; Vecera and O'Reilly, 1998; Zhaoping, 2005). There is no empirical evidence that V1 contains separate sub-populations of neurons responding to texture edges and boundary edges. However, if such neurons did exist they would have similar RFs, and hence, similar response properties and would be unlikely to be classified separately unless such distinctions were being actively sought.

The lateral weights in the PC/BC model of V1 are illustrated in Fig. 4. The lateral connections between prediction neurons representing boundary edges preferentially connect prediction neurons with feedforward RFs at locations and with orientations consistent with a smooth, co-circular, contour joining those RFs. Texture-to-boundary connections are defined so that prediction neurons selective for boundary edges are excited by texture elements that are roughly perpendicular. Texture-to-texture connections are defined so that the strongest connections are between prediction neurons that have roughly parallel RFs. Boundary-to-texture connections are defined so that prediction neurons selective for texture edges are excited by boundary elements that are roughly perpendicular. The lateral connections between prediction neurons representing boundaries are consistent with co-circularity. Such connections are consistent with natural image statistics (Geisler et al., 2001; Sigman et al., 2001), and are believed to be encoded by long-range horizontal connections in V1 (Field et al., 1993; Fitzpatrick, 2000; Hess et al., 2003; Hunt et al., 2011). The lateral weights to and from prediction neurons representing texture elements are anti-correlated with co-circularity. Both these types of connections are seen in cortex (Hunt et al., 2011). The pattern of lateral connectivity between boundary-edge detecting prediction neurons is similar to that used in many previous models of contour detection (*e.g.*, Ben-Shahar and Zucker, 2004; Hansen and Neumann, 2008; Huang et al., 2009; Li, 1998; Mundhenk and Itti, 2005; Parent and Zucker, 1989; Ursino and La Cara, 2004; Vonikakis et al., 2006; Yen and Finkel, 1998).

2.4 PC/BC as a Model of Attention

Previous work with hierarchical versions of PC/BC has proposed that top-down connections (connections from one stage in a hierarchy of processing stages to a preceding stage) should be implemented using a distinct type of connection which generates modulatory affects via multiplication. Such distinct, multiplicative, top-down connections have been used to simulate the modulatory effects of attention (De Meyer and Spratling, 2009; Spratling, 2008a). However, given that modulatory effects can be generated in the PC/BC model without the need for additional mechanisms, this raises the intriguing possibility that modulatory, top-down, affects could be generated using the same mechanism as is used to integrate feedforward and lateral connections, as described in the preceding sections.

To simulate the effects of attention (see section 3.4) an architecture like that shown in Fig. 2 is used. One

set of inputs are sensory-driven while the other set of inputs provide attentional biases. Both sets of inputs are integrated identically. There is strong evidence that attentional influences are transmitted via cortical feedback pathways (Buffalo et al., 2010; Desimone and Duncan, 1995; Mehta et al., 2000b; Pollen, 1999; Schroeder et al., 2001; Spratling and Johnson, 2004; Treue, 2001). The proposed model is therefore intended to simulate the effects that cortical feedback connections have on neural response properties. However, as the models treats all inputs identically, the same model could also simulate the effects of attentional signals that are transmitted via the thalamus (Shipp, 2004). How such attentional signals are generated (*e.g.*, by short-term memory, task demands, *etc.*), or where they are generated (*e.g.*, parietal cortex, pre-frontal cortex, superior colliculus, *etc.*) is not addressed by the current model. Here, we only consider the effects of attention on the processing of sensory signals in the early stages of the cortical visual pathway, rather than considering how and where attentional signals originate (Corbetta and Shulman, 2002; Kastner and Ungerleider, 2000; Shipp, 2004; Their et al., 2002).

The weights connecting the attentional inputs to the prediction neurons are defined using a Gaussian function. Hence, attentional input is distributed to a sub-population of prediction neurons, with the strength of attention falling with distance, providing a "spot-light" of attention, as is typically used in other models of attention. To model spatial attention, the Gaussian function used to define the weights is narrowly tuned to spatial location, but widely tuned to the stimulus preference of the prediction neurons. Hence, spatial attention provides input to all prediction neurons in the same spatial region, irrespective of the tuning of those neurons to different sensory inputs. In contrast, to model featural attention, the Gaussian function that is used to define the weights is widely tuned to spatial location, but narrowly tuned to the stimulus preference of the prediction neurons. Hence, featural attention provides input to all prediction neurons tuned to similar stimulus features, irrespective of the RF location of those neurons.

2.5 Code

Software, written in MATLAB, which implements the algorithm described in the preceding sections, and performs the simulations described in the following sections, is available at:
`http://www.corinet.org/mike/Code/drivers_modulators.zip`.

3 Results

3.1 Feedforward driving and modulatory influences

Figure 5 provides a simple illustration of how feedforward connections in the PC/BC model can give rise to both driving and modulatory influences. This PC/BC network has the architecture shown in Fig. 1a. In Fig. 5a both inputs to the single output (prediction) neuron can independently drive a response: either input can evoke a significant response in the absence of any other inputs. In more realistic models sets of inputs, rather than individual inputs, would typically need to be co-active to drive the response of a prediction neuron. In Fig. 5b the upper-most input to the top prediction neuron is modulatory while the second input is driving. In both Fig. 5a and Fig. 5b the upper-most prediction neuron is wired-up identically and it integrates all the inputs it receives identically. The crucial difference is that in Fig. 5b the upper-most input is also connected to many other prediction neurons (as indicated by the dashed connections). If we think about the inputs as providing evidence to support hypotheses represented by the prediction neuron responses, then when the first input is active in isolation (the situation illustrated in the left column of Fig. 5b), this provides evidence to equally support many hypotheses, and hence, all of these alternative interpretations of the evidence are equally weakly active. In contrast, when the first and second inputs are active simultaneously (the situation illustrated in the right column of Fig. 5b), then the additional evidence supporting the hypothesis represented by the upper-most prediction neuron causes the activation dynamics of the PC/BC network to choose this as the most likely hypothesis, and the evidence for the alternative hypotheses is explained away (Kersten et al., 2004; Lochmann and Deneve, 2011) suppressing the responses of the other prediction neurons and allowing all the evidence supplied by the first input to support the hypothesis represented by the upper-most prediction neuron. The uppermost input to the network shown in Fig. 5b thus has a modulatory influence on the uppermost prediction neuron. This influence is facilitatory. An alternative way of thinking about how inputs are integrated by the prediction neurons in a PC/BC network is to consider each input as providing a fixed amount of activation which is distributed among the active prediction neurons to which it connects (Achler and Amir, 2008; Reggia, 1985). Hence, if an input connects to many active prediction neurons, its drive will be shared between those neurons, and it will cause very little additional activation to any one of them. However, if the number of active predictions neurons is small, the input is distributed less thinly, and has a greater effect. In the limit, if there is only one active prediction neuron this will receive all the input, and hence, its response can be strongly influenced.

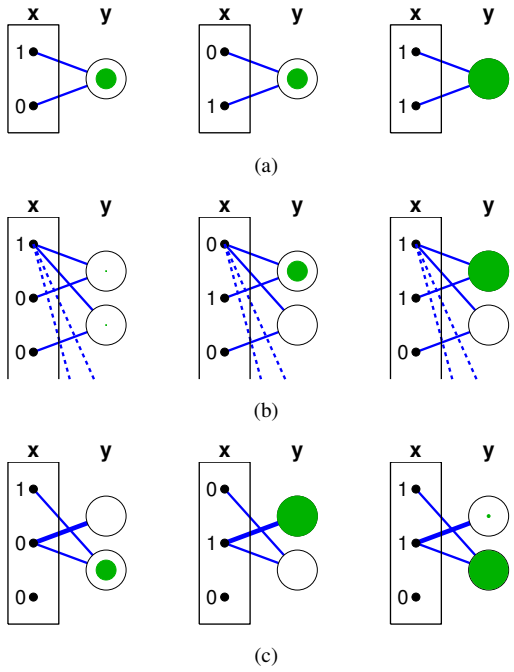

Figure 5: Driving and modulatory influences in feedforward connectivity. Each sub-figure shows a simple PC/BC neural network. For each network the output of the prediction neuron(s), labelled $\mathbf{y}$, are shown for different combinations of input stimuli, labelled $\mathbf{x}$. The strength of each prediction neuron's response is indicated by the diameter of the shading (the shading is the same diameter as the circle when the response is equal to one). For clarity, the error-detecting neurons in each PC/BC network (see section 2) have been omitted from these diagrams, as have the one-to-one connections from the inputs to the error-detecting neurons. The connections shown between the inputs and the prediction neurons represent the synaptic weights $\mathbf{W}$, with the thickness of the connection being proportional to the strength of the corresponding weight. In (a) there are two inputs and one prediction neuron. This neuron receives equally weighted connections (with strength 0.5) from each of the two inputs. In this case, both inputs have the same influence on the output, producing an output equal to approximately 0.5 when either input is presented in isolation and an output of approximately one when both inputs are presented simultaneously. In (b) there are 21 inputs and 20 prediction neurons, but for clarity only the first three inputs and first two prediction neurons are shown: all additional inputs have a value of zero in each simulation, and all other prediction neurons produce identical responses to that shown for the second (lower) prediction neuron. The first (upper-most) prediction neuron is wired-up exactly as the prediction neuron in (a). The additional prediction neurons also each receive equally weighted connections (with strength 0.5) from two inputs: all receive one of these connections from the first input (indicated by the dashed connections), and the other connection from a unique input. In this case, the first input to the first prediction neuron is modulatory while the second input is driving. Specifically, when the first input is active in isolation the first prediction neuron output is very weak (approximately 0.025 in this specific example), whereas, when the second input is active in isolation the prediction neuron response is much stronger (approximately 0.5). When both inputs are simultaneously active the output of the prediction neuron is approximately one. In (c) there are three inputs and two prediction neurons. This upper-most prediction neuron receives a connection (with weight 1) from the second input, while the bottom-most prediction neuron receives equally weighted connections (with strength 0.5) from each of the two first two inputs. As in (b), the first input to the first prediction neuron is modulatory while the second input is driving. However, in this example, the modulatory influence is suppressive rather than facilitatory. Specifically, when the first input is active in isolation the first prediction neuron output is approximately zero, whereas, when the second input is active in isolation the upper-most prediction neuron response is strong (approximately one). When both inputs are simultaneously active the output of the first prediction neuron is again approximately zero.

Explaining away causes suppressive modulation which is more clearly seen in Fig. 5c. Here, the first input is not connected to the upper most prediction neuron, and hence, it has no influence on the response of this neuron when presented in isolation (as illustrated in the left column of Fig. 5c). The second input is the driver for the first prediction neuron, the situation illustrated in the middle column of Fig. 5c. However, when the first input is presented simultaneously with this driving stimulus, the pattern of input stimulation is more accurately represented by the second prediction neuron. The second prediction neuron is thus made active by the dynamics of the PC/BC network, and the input to the first prediction neuron is explained away. The uppermost input to the network shown in Fig. 5c thus has a modulatory influence on the uppermost prediction neuron. This influence is suppressive.

Larger-scale neural networks, implemented using matrix multiplication (as illustrated in Fig. 1a) or filtering (as illustrated in Fig. 1b), have been shown in previous work to successfully simulate the response properties of orientation tuned cells in primary visual cortex (Spratling, 2010, 2011, 2012a,b). Specifically, the PC/BC model of V1 (without lateral connections) has been shown to simulate modulatory influences on V1 response properties, including: surround suppression (see Spratling, 2010, Figs. 5b, 5c, 9, 10, Spratling, 2011, Figs. 4, 5, 6, and 7 and Spratling, 2012b, Fig. 15b); the effects of flankers and textured surrounds (see Spratling, 2010, Fig. 11); and shifts in orientation tuning caused by the orientation of a preceding stimulus (see Spratling, 2012a, Fig. 6).

In this previous work, the response of a simulated V1 neuron is driven by a stimulus (of approximately the correct orientation, phase, and spatial frequency) appearing in the centre of its RF. However, this response can be modulated by stimuli appearing at surrounding locations; simulating both the suppressive and facilitatory influences of V1 ncRFs (Angelucci and Bullier, 2003; Jones et al., 2001; Kapadia et al., 2000; Seriès et al., 2003). The modulatory influences of the surround in the PC/BC model are due to the encroachment of stimulus into the periphery of the prediction neuron's feedforward RF. The weights at the periphery of the RF are weak. A location at the periphery also forms part of the feedforward RF of many other neurons. Hence, if the periphery is stimulated in isolation, it may weakly activate many neurons, and have a negligible influence on the response of the recorded neuron (analogous to the situation shown on the left of Fig. 5b). Alternatively, the peripheral stimulus may be the driving stimulus for another neuron, in which case when the periphery is stimulated in isolation it may drive the response in this second neuron and again have a negligible influence on the response of the recorded neuron. In contrast, if the surround is stimulated simultaneously with the centre, the weak input from the surround can have a facilitatory affect on the recorded neuron's response (analogous to the situation shown on the right of Fig. 5b). Alternatively, if the stimulus in the surround is a driver of the response in another neuron, with an overlapping RF, then this other neuron will also be activated and will compete with the recorded neuron, suppressing its response (analogous to the situation shown on the right of Fig. 5c).

Other previous work has shown that feedforward PC/BC networks which receive inputs from distinct sources, as illustrated in Fig. 2, can produce responses that are driven by one set of inputs and modulated by the other. This has been used to simulate gain modulation as is observed in various cortical areas, for example, when a retinal RF is modulated by eye position (De Meyer and Spratling, 2011, in p).

3.2 Lateral driving and modulatory influences

All the simulations reported in this section explore the influence of lateral connections in the PC/BC model, and were performed using the architecture illustrated in Fig. 3.

Figure 6 provides a simple illustration of how recurrent connections in the PC/BC model can give rise to both driving and modulatory influences. In each simulation, the upper-most prediction neuron provides recurrent input to the network. This recurrent input is shown as the bottom-most input on the left of each network. In Fig. 6a the second input and the bottom-most (recurrent) input can independently drive a response from the second (bottom-most) prediction neuron. In Fig. 6b the bottom-most (recurrent) input has a modulatory effect on the response of the second prediction neuron. In both Fig. 6a and Fig. 6b the second prediction neuron is wired-up identically and it integrates the inputs it receives identically. The crucial difference is that in Fig. 6b the recurrent input is also connected to many other prediction neurons (as indicated by the dashed connections). As described previously when discussing the simulations shown in Fig. 5b, the high fan-out of connections from the recurrent input causes its influence to become modulatory. Hence, in an identical way to the feedforward inputs, recurrent inputs can have either a driving or modulatory influence on prediction neuron responses.

Indeed, the behaviour of the second prediction neuron in Fig. 6a is equivalent to the behaviour of the prediction neuron in Fig. 5a. Similarly, the behaviour of the second prediction neuron in Fig. 6b is equivalent to the behaviour of the first prediction neuron in Fig. 5b. Furthermore, if we ignore the upper-most input and upper-most prediction neuron in each network shown in Fig. 6, the circuits shown in Figs. 5 and 6 are identical. This means that recurrent PC/BC networks could be implemented as a hierarchy of processing stages, with the recurrent connections replaced by feedforward connections. These alternative implementation strategies are not necessarily mutually exclusive: cortical circuitry might well use both.

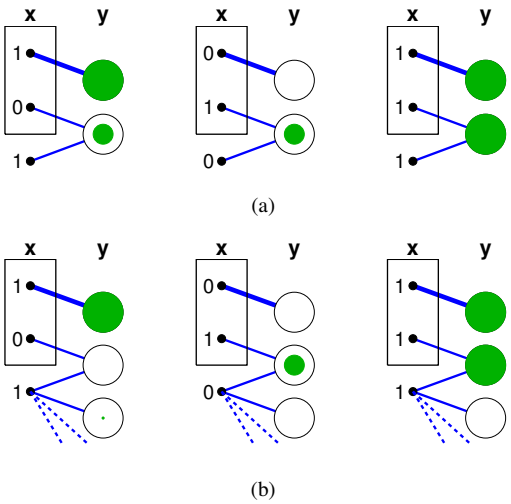

Figure 6: Driving and modulatory influences in recurrent connectivity. Each sub-figure shows a simple PC/BC neural network in which the outputs provide additional, recurrent, inputs to the network. Recurrent inputs are on the left, but outside the box labelled $\mathbf{x}$. For clarity, only the recurrent input from the upper-most prediction neuron is shown: the recurrent inputs from other prediction neurons do not affect the results. The format of the diagram is thus equivalent to Fig. 3a, however, for clarity, the error-detecting neurons in the PC/BC networks have been omitted from these diagrams. For each network the output of the prediction neurons, labelled $\mathbf{y}$, are shown for different combinations of feedforward input stimuli, labelled $\mathbf{x}$ (from left to right the inputs are $[1,0]^T$, $[0,1]^T$, and $[1,1]^T$). The strength of each prediction neuron's response is indicated by the diameter of the shading (the shading is the same diameter as the circle when the response is equal to one). In (a) there are two inputs and two prediction neurons. The lower prediction neuron neuron receives equally weighted connections (with strength 0.5) from the second input and the recurrent input provided by the upper-most prediction neuron. This recurrent connection enables the first input, which drives the response of the upper-most prediction neuron, to also drive the response of the second prediction neuron. In (b) there are 20 prediction neurons, but for clarity only the first three prediction neurons are shown: all other prediction neurons produce identical responses to that shown for the third (lower) prediction neuron. The second (middle) prediction neuron is wired-up exactly as the second prediction neuron in (a). The additional prediction neurons also each receive equally weighted connections (with strength 0.5) from two inputs: all receive one of these connections from the recurrent input provided by the upper-most prediction neuron (indicated by the dashed connections), and the other connection from a unique recurrent input. In this case, the recurrent input provided by the upper-most prediction neuron to the second prediction neuron is modulatory. Specifically, it causes little response when presented in isolation, but has a a significant facilitatory effect on the response of the second prediction neuron when the second input is also active.

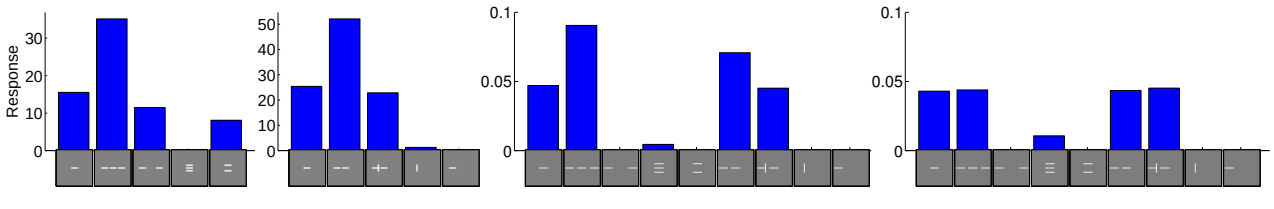

Figure 7: The effect of flankers on neural response. (a) Response to one set of flanker configurations of a single cell in primate V1 (adapted from Kapadia et al., 2000, Fig. 7a). (b) Response to a second set of flanker configurations of a different cell in primate V1 (adapted from Kapadia et al., 1995, Fig. 11a). (c) and (d) Response of a model neuron to both sets of flanker configurations shown in (a) and (b): (c) with lateral connections, (b) without lateral connections.

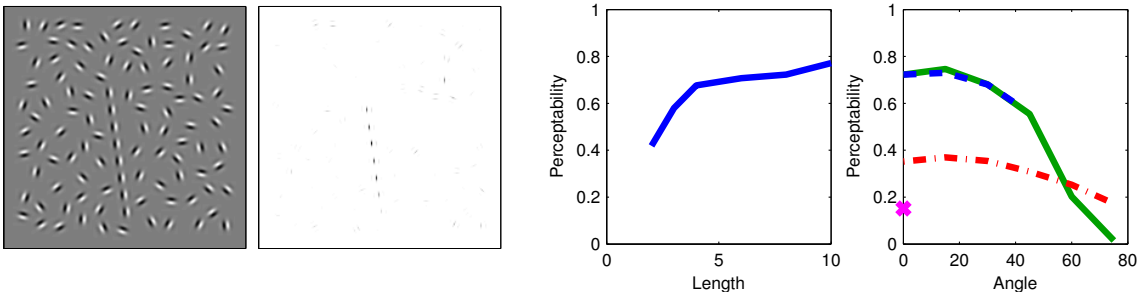

(a) (b) (c) (d)

Figure 8: Modulatory influences of lateral connectivity in the PC/BC model of V1 when applied to contour integration tasks. (a) a typical stimulus used to assess contour integration in humans. (b) the response of boundary-edge detecting prediction neurons in the PC/BC model of V1 with lateral connections, when presented with the stimulus in (a). The maximum response across prediction neurons tuned to different orientations is shown at each location, with darker pixels corresponding to stronger responses. (c) Simulation results showing contour perceptibility measured in the PC/BC model as a function of path length for straight paths. (d) Simulation results showing contour perceptibility measured in the PC/BC model as a function of the angle between adjacent elements in 8 element long paths. The solid line shows results for non-smooth paths, the dashed line shows results for smooth paths, the dash-dot line shows results for snakes, and the cross shows the result for a straight path made up of elements angled at 45 degrees to the direction of the path.

A canonical example of the modulatory influences of lateral connections in cortex is provided by experiments exploring the influences of flanker stimuli on the response properties of orientation selective neurons in V1 (Chen et al., 2001; Kapadia et al., 1995, 2000; Mizobe et al., 2001; Polat et al., 1998). These modulatory influences are widely believed to be mediated by long-range horizontal connections in the superficial layers of V1 (Angelucci and Bressloff, 2006; Seriès et al., 2003). Typically, a pair of collinear flankers, or a single collinear flanker, increases the response to a bar presented at the center of the RF, even though these flanking stimuli produce little response when presented alone (see Fig. 7a and b). Furthermore, the enhancement due to a collinear flanker can be blocked by a perpendicular bar separating the central bar from the flanker (see Fig. 7b). In contrast to collinear flankers, parallel flankers suppress the response to the central bar (see Fig. 7a).

These results can be simulated using the PC/BC model of V1 with lateral connections. The simulation results are shown in Fig. 7c. The modulatory effects of the lateral connections can be clearly seen if these results are compared to those generated when the lateral connections are removed from the model as shown in Fig. 7d. Without the lateral connections collinear flankers have little affect on the response of the recorded prediction neuron. Using the PC/BC model of V1 it has previously been shown that when the images are sufficiently small so that the flankers encroach on the periphery of the feedforward RF of the recorded neuron, similar modulatory effects can be produced without recurrent connectivity (see Fig. 11f in Spratling, 2010). For the results presented in Fig. 7 the stimuli are larger, so that the flankers do not stimulate the periphery of the recorded neuron's feedforward RF. The similarity of the results presented here (showing the modulatory influences of lateral connections) and the previous results (showing the modulatory influences of feedforward connections), suggest that either (or both) forms of connectivity might give rise to the modulatory influences of flankers observed in cortex.

Lateral connectivity in V1 is widely believed to give rise to the perceptual grouping of image elements forming contours (Hess and Field, 1999; Hess et al., 2003; Loffler, 2008). This phenomenon has been extensively explored using images of Gabor patches in which certain patches are aligned to form a path amongst randomly oriented distractors, an example of such a stimulus is shown in Fig. 8a. Figure 8b shows the response of the boundary-edge detecting prediction neurons in the PC/BC model of V1 to the image shown on the left. It can be seen that the lateral connections in the PC/BC model result in stronger responses from those prediction neurons representing path elements compared to those elements representing distractor elements. This contour integration paradigm has been used extensively to study the ability of human subjects to perceive the path among the distractors. In order to simulate this data it is necessary to define a measure of the model's behaviour which correlates with contour perceptibility. For this purpose, the mean response of all neurons responding to path elements (R_p) is compared to the mean response of neurons responding to distractor elements (R_d). Specifically, a perceptibility index is calculated as $PI = \frac{R_p - R_d}{R_p + R_d}$. This value is calculated separately for the boundary edge detecting prediction neurons and the texture edge detecting neurons, and the overall perceptibility of the contour is taken as the max of these two measures. For each experimental condition, this measure of perceptibility was calculated for 25

Figure 9: Modulatory influences of lateral connectivity in the PC/BC model of V1 when applied to boundary detection in natural images. The top row shows three images taken from the RuG dataset (Grigorescu et al., 2003). The bottom row shows the boundary edges detected by the PC/BC model of V1 with lateral connections.

randomly generated images, and the mean value was used as a measure of the perceptibility of contours in these images.

For human observers, contour detection improves as the number of elements forming the path increases (Braun, 1999; Li and Gilbert, 2002; Watt et al., 2008). Figure 8c shows similar results for the PC/BC model. For humans, contour detection performance reduces as the curvature of the path increases (Dakin and Hess, 1998; Field et al., 1993). The model produces similar behaviour (Fig. 8d). However, in the model performance is identical for smooth contours (in which the change in angle between adjacent path elements is identical) and non-smooth contours (in which the sign of the change in angle between adjacent path elements varies randomly). This is not consistent with the psychophysical results, which show that performance is poorer for non-smooth paths (Hess et al., 2003; Pettet, 1999). Human contour integration performance is highest when the path elements are aligned with the local contour orientation (to form snakes), performance is poorer for path elements aligned perpendicularly to the local contour orientation (to form ladders), and is worst when the path elements make an angle of 45 degrees to the contour direction (Dakin and Baruch, 2009; Field et al., 1993; Ledgeway et al., 2005). The model produces similar behaviour (Fig. 8d). However, for the model the perceptibility of snakes is less sensitive to path angle than is the case for the psychophysical data (Field et al., 1993).

The current model of V1 employs patterns of lateral connectivity that are similar to several previous models. It is therefore not particularly surprising that it can account for similar data, and that it has similar limitations as those previous models. However, what is surprising is that in the current model the lateral inputs are integrated in exactly the same way as the feedforward input. Despite this, lateral connections have modulatory influences while feedforward inputs are driving. For example, in Fig. 7c the collinear flankers provide the same lateral input to the recorded neuron in both the second and third stimulus configurations. When there is no central bar, this lateral input is ineffective at modifying the response of the recorded neuron. However, it does have a strong affect on the response when the central bar is present. Similarly, in Fig. 8 many prediction neurons are activated by the Gabor patches, and each of these neurons is providing lateral input to other prediction neurons in its neighbourhood. However, rather than spreading activation indiscriminately, the lateral connections only modulate the strength of the response of the prediction neurons receiving driving feedforward input.

In addition to being able to account for neurophysiological and psychophysical data, the PC/BC model of V1 with lateral connections also has practical applications. The model is affective at extracting perceptually salient

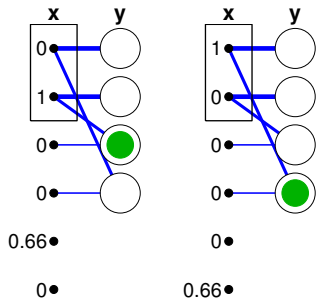

Figure 10: Temporal influences of recurrent connectivity: motion detection. Each sub-figure shows a simple PC/BC neural network in which the outputs provide additional, recurrent, inputs to the network. Recurrent inputs are on the left, but outside the box labelled $\mathbf{x}$. Note that in this example two of the recurrent inputs are not connected to any of the prediction neurons. The output of the prediction neurons, labelled $\mathbf{y}$, are shown for different temporal sequences of feedforward input stimuli, labelled $\mathbf{x}$. The strength of each prediction neuron's response is indicated by the diameter of the shading (the shading is the same diameter as the circle when the response is equal to one). If the two feedforward inputs to the network are labelled "a" and "b", then the temporal sequences of inputs used were (left) "ab" and (right) "ba". The activity of the neurons in the network is shown at the end of the input sequence. For clarity, the error-detecting neurons in the PC/BC networks have been omitted from these diagrams.

boundaries in natural images. Some example results are shown in Fig. 9. The proposed algorithm is currently limited to using only intensity information at a single scale. However, it has been shown to out-perform the current state-of-the-art machine vision image segmentation method (Pb) when this method is also restricted to using the same information (Spratling, 2013).

3.3 Temporal influences

The architecture illustrated in Fig. 3 was also used to perform all the simulations described in this section.

Figure 10 provides a simple illustration of how recurrent connections in the PC/BC model can give rise to driving influences in the temporal domain. In each simulation, the four prediction neurons provide recurrent input to the network. This recurrent input is shown as the four lower inputs on the left of each sub-figure. The network distinguishes two sequences of input stimulation. The third prediction neuron responds when the sequence of inputs is the top-most input followed by the second input (Fig. 10left). The fourth prediction neuron responds when the temporal sequence of the inputs is reversed (Fig. 10right). If the inputs to this network came from appropriately positioned sensors, it could be used to encodes direction of motion: *e.g.*, to distinguish leftward motion from rightward motion. Direction selectivity is achieved because the recurrent inputs to the third and fourth prediction neurons are delayed by the integration time of the two prediction neurons (the first and second) which are providing the recurrent stimulation. In this respect, the current model is similar to previous models of direction selectivity which all employ a time delay between inputs that are spatially offset (Adelson and Bergen, 1985; Barlow and Levick, 1965; Rao and Sejnowski, 1999; Reichardt, 1961). The exact cortical mechanism implementing this time delay is yet to be fully resolved (Baker and Bair, 2012). As discussed at the beginning of section 3.2, recurrent PC/BC networks could be alternatively implemented as a hierarchy of processing stages. In this case the delay required for motion detection could be implemented via differences in transmission speed in feedforward connections.

Figure 11 shows a slightly more complex model of temporal sequence processing. Here the network is wired up so that seven prediction neurons provide recurrent input to the network. The last four of these prediction neurons respond to distinct (three element long) sequences of inputs. The first four prediction neurons are wired-up as in Fig. 10. Hence, if the two feedforward inputs to the network are labelled "a" and "b", the third prediction neuron responds to the sequence of input "ab", while the fourth prediction neuron responds to the sequence "ba". The last four prediction neurons each receive recurrent input from either the third or fourth prediction neurons, as well as feedforward connections from one of the two inputs. This enables the last four prediction neurons to distinguish longer sequences of inputs, specifically: "aba", "abb", "baa", and "bab". It would be possible for another neuron to receive recurrent input from one of the last four prediction neurons as well as one of the feedforward inputs, in order to represent an even longer sequence.

As well as having driving influences on prediction neuron responses, lateral connections can also have modulatory influences. In the temporal domain, this can give rise to earlier or stronger responses to stimuli. A simple

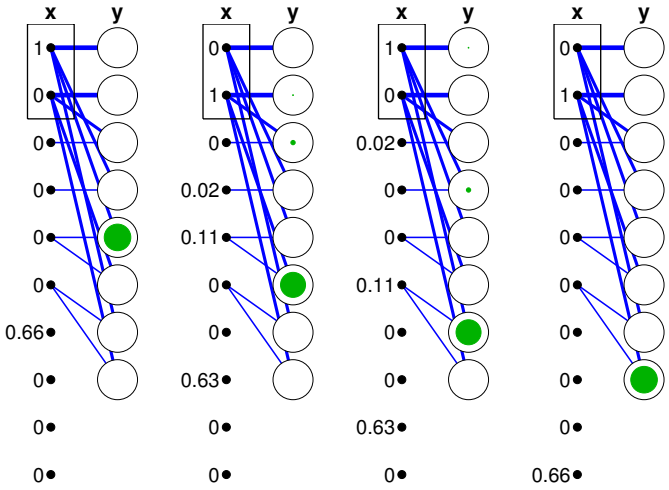

Figure 11: Temporal influences of recurrent connectivity: sequence representation. The format of this figure is identical to, and described in the caption of, Fig. 10. Note that in this example the bottom two recurrent inputs are not connected to any of the prediction neurons. If the two feedforward inputs to the network are labelled "a" and "b", then the temporal sequences of inputs used were, from left to right: "aba", "abb", "baa", and "bab".

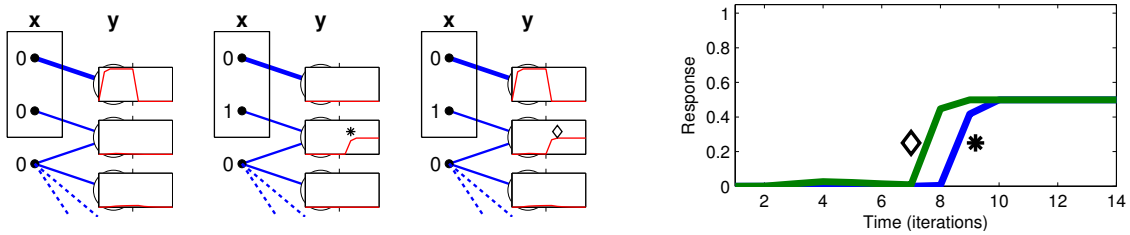

(a) (b)

Figure 12: Temporal influences of recurrent connectivity: priming. (a) The format of this figure is identical to, and described in the caption of, Fig. 10, except that rather than showing the activity of the prediction neurons at the final iteration, the graphs superimposed on each node show the activation of the corresponding prediction neuron through time. All these graphs have axes that are scaled identically. The circuit used for this simulation is identical to that used in the simulation shown in Fig. 6b. The only difference if that the inputs are presented in sequence, rather than simultaneously. If the two feedforward inputs to the network are labelled "a" and "b", and the absence of any input is labelled "–", then the temporal sequences of inputs used were, from left to right: a–, –b, and ab. In this case, the recurrent input provided by the upper-most prediction neuron to the second prediction neuron primes the response of the second prediction neuron, causing the second prediction neuron to respond earlier when the second input is presented after the first input. (b) The two temporal response curves marked with the asterisk and the diamond in (a) are shown enlarged on the same axes to allow the effect of priming to be more clearly seen.

illustration of this priming effect is provided in Fig. 12. In the right-hand sub-figure of Fig. 12a, the first input is active for 7 iterations and for the following 7 iterations, the second inputs is active. The response of the second prediction neuron is driven by the appearance of the second input. However, if this response is compared to that which is generated when the second input is not preceded by the first input (as shown in the middle sub-figure of Fig. 12a) it can be seen that the first input causes the second prediction neuron to respond more quickly to the appearance of the second input.

Spatio-temporal influences on the responses of neurons in cortical area V1 were investigated by Guo et al. (2007). Stimuli consisted of sequences of bars appearing at different image locations, with the final bar appearing within the classical receptive field (cRF) of the recorded neuron (see Fig. 13). In one experimental condition the sequence of bars was predictive of the orientation of the final bar presented to the cRF. In another condition the

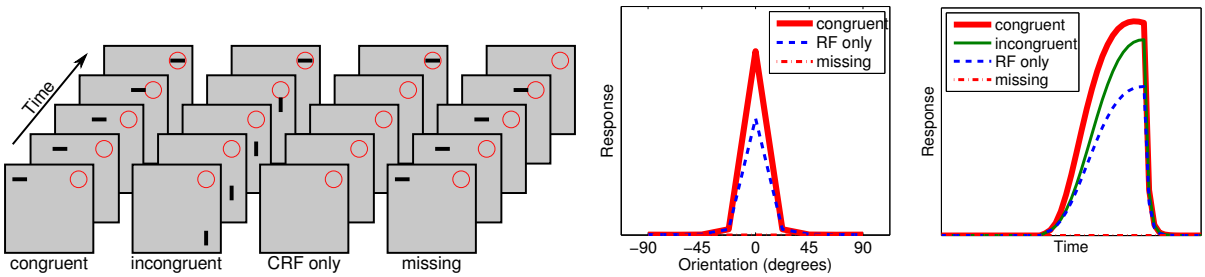

(a) (b) (c)

Figure 13: Modulatory influences of lateral connectivity in the PC/BC model of V1 when applied to the spatio-temporal prediction of a moving stimulus. (a) Experimental conditions. Each shaded square shows an image, the circles indicate the location of the RF of the recorded neuron and were not present in the stimulus. A sequence of moving bars were either: predictive of the orientation of the bar appearing within the RF of the recorded neuron ("congruent" condition); not predictive of the orientation of the bar appearing in the RF of the recorded neuron ("incongruent" condition); missing, so that only the RF stimulus was presented ("RF only" condition); or were followed by a blank image ("missing" condition). (b) Simulation results showing orientation tuning of the recorded neuron. (c) Simulation results showing the response over time of the recorded neuron.

bar was presented to the cRF without being preceded by a sequence of moving bars. In both the physiological experiments (Guo et al., 2007) and the simulation results (Fig. 13b) the same orientation tuning was recorded with and without a predictive sequence. In the physiological experiments it was also found that some neurons had early response to predictive stimuli. That is they responded, with the same orientation tuning, but with reduced strength, to the predictors (particularly the last predictor) without any stimulus appearing in the cRF. If the predictive influences are mediated by lateral connection in V1, then this result suggests that those lateral connections can drive a response in the absence of cRF stimulation. This suggests that for the PC/BC model of V1 the fan-out of the lateral connections is too great: less fan-out would allow lateral connections to have more of a driving influence.

In another experimental condition the bars in the sequence had a different orientation to the bar presented to the cRF, and hence, the sequence was not predictive of the orientation of the final bar. Analysis of the physiological data (Guo et al., 2007) showed that information about the orientation of the target was reduced and had a longer latency in this incongruent condition compared to the congruent condition in which the sequence was predictive. Similarly, the simulation results (Fig. 13c) show that response of the neuron tuned to the stimulus presented in the cRF is stronger and has a reduced latency in the congruent compared to the incongruent condition.

3.4 Attentional influences

Attention modulates the sensory-driven activation of cortical cells (Kanwisher and Wojciulik, 2000; Kastner and Ungerleider, 2000; Luck et al., 1997) and is probably the domain in which modulatory influences on cortical response properties have been most widely studied. As a simple model of these attentional influences a PC/BC model with the architecture shown in Fig. 2 was used. One set of inputs acted as the source of attentional influences while the other set of inputs were sensory-driven. For convenience, the sensory RFs were defined exactly as for the PC/BC model of V1, such that neurons showed orientation tuning. No lateral connections were used for these simulations. The connections weights from the attentional inputs were defined using Gaussians to define both spatial and featurally selective "spot-lights" of attention.

For both spatial and featural attention, the weights from the attentional inputs had a large fan-out. Hence, in the absence of a visual stimulus an attentional input provides weak support for a wide range of different hypotheses about the stimulus. However, this attentional input reduces the range of possible hypotheses compared to conditions in which there is no attention. When sensory-driven inputs are presented, the attentional inputs are integrated with the sensory evidence to bias the perceptual inference carried out by the PC/BC processing stage. Endogenous attention in this model is therefore a mechanism that guides perceptual inference by providing priors that are more specific to the expected stimulus. In this view, endogenous attention is just another consequence of performing perceptual inference rather than a specialised mechanism for limiting access to processing resources.

The effects of spatial attention on the tuning response functions of single cells has been investigated for direction tuning in cortical area MT (Treue and Martinez-Trujillo, 1999), and for orientation tuning in cortical areas

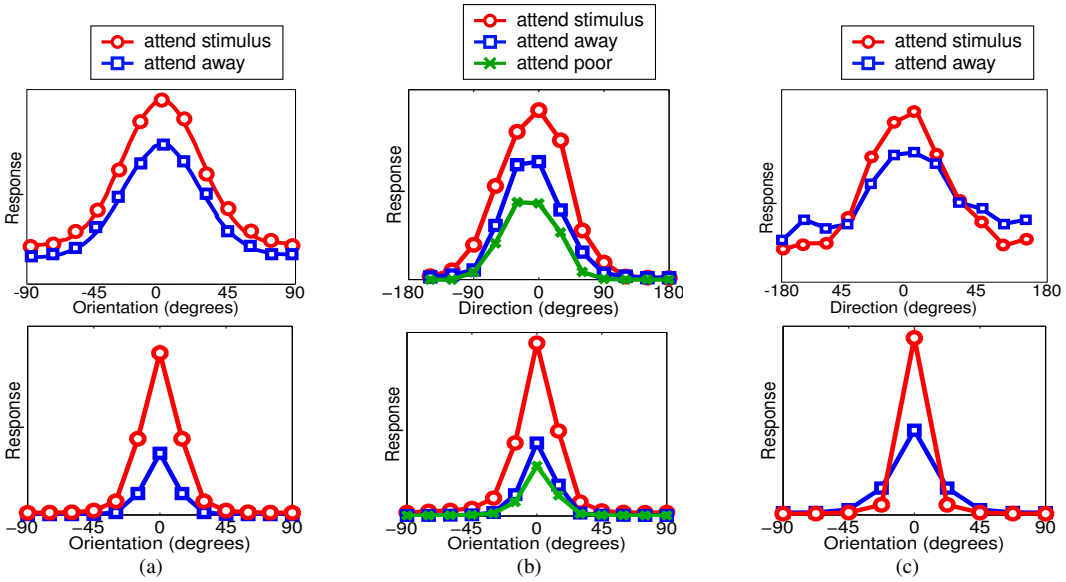

Figure 14: Attentional influences on tuning response functions. Top row shows neurophysiological data, bottom row shows corresponding simulation results. (a) Effects of spatial attention on tuning for a single stimulus. Neurophysiological data showing average tuning curves measured in V4 (adapted from McAdams and Maunsell, 1999a). (b) Effects of spatial attention on tuning for a pair of stimuli. Neurophysiological data showing average tuning curves measured in MT (adapted from Treue and Martinez-Trujillo, 1999). (c) Effects of featural attention on tuning. Neurophysiological data showing the response of a single neuron in MT (adapted from Martinez-Trujillo and Treue, 2004).

V1, V2 and V4 (McAdams and Maunsell, 1999a; Motter, 1993). All of these experiments found similar effects. In these experiments, a single stimulus was presented within the receptive field and the response of the neuron was recorded as the direction of motion or orientation of this stimulus was varied. It was found that when attention was directed to the location of the stimulus, the recorded cell's response was enhanced compared to when attention was directed to a different location (see Fig. 14a). The effect of attention was a multiplicative scaling of the tuning response function. In the PC/BC simulation, for each attentional state the attentional input is the same for all orientations of the stimulus. However, despite the attentional input being constant it generates almost perfect multiplicative modulation of the response. Hence, the results for the PC/BC model are similar to the neurophysiological data (see Fig. 14a).

Treue and Martinez-Trujillo (1999) also tested the effects of spatial attention on the direction tuning of cells in cortical area MT when there were two stimuli within the RF. The response of a neuron was recorded as the direction of motion of one of the stimuli in its RF was varied. The second stimulus in the recorded neuron's RF had a fixed direction of motion in the cell's non-preferred direction. Three attentional conditions were used: one where attention was directed to the stimulus with the varying direction of motion, one where attention was directed to the non-preferred stimulus, and one where attention was directed away from the RF. Compared to the tuning function measured when attention was directed away from the RF, attention to the varying stimulus increased response while attention to the non-preferred stimulus reduced response (see Fig. 14b). Similar results were produced by the PC/BC model using orientation tuning as a surrogate for direction of motion tuning (see Fig. 14b).

A similar experiment was performed by Martinez-Trujillo and Treue (2004) to determine the effects of featural attention on the direction of motion tuning of cells in areas MT. In this experiment a single moving random dot pattern was presented within the RF of the recorded cell. By varying the direction of motion of the stimulus relative to the recorded cell's preferred direction, tuning curves were generated for two attentional conditions. In the first condition, attention was directed to a stationary fixation point outside the RF of the recorded neuron (*i.e.*, direction of motion was ignored). In the second condition attention was directed to a second moving random dot pattern outside the RF of the recorded neuron which had the same direction of motion as the pattern within the recorded cell's RF (*i.e.*, attention was directed to the same direction of motion as the stimulus). It was found that attention caused an enhancement of the cell's response when the direction of motion was close to the preferred direction for the cell, but a suppression of response when the direction of the stimulus (and hence the attended direction) was far from the cell's preferred direction (see Fig. 14c). Again, similar results were produced by the

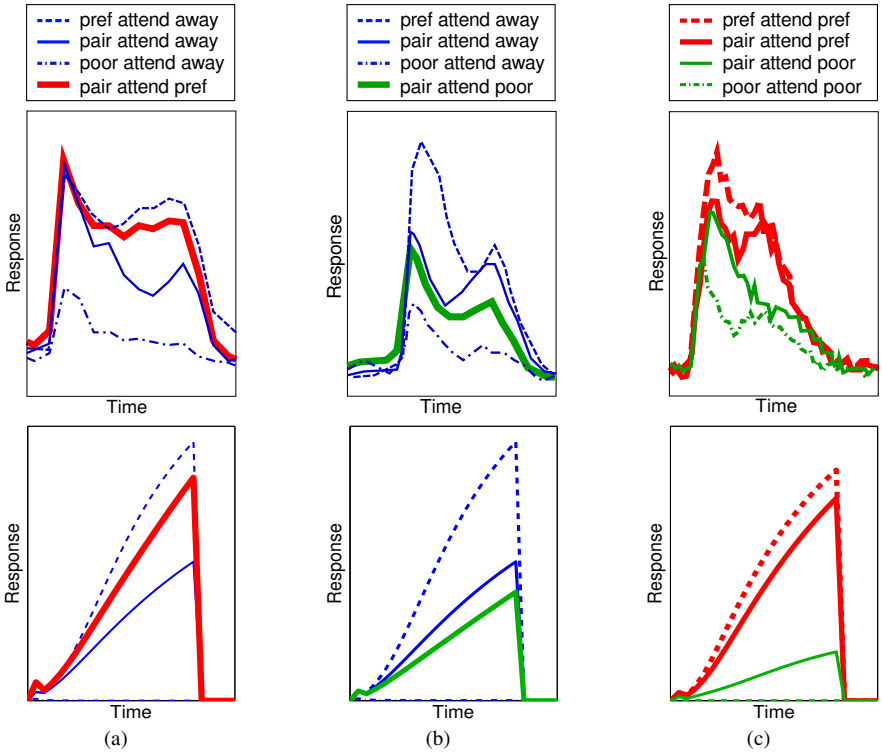

Figure 15: Attentional influences on neural responses. Top row shows neurophysiological data, bottom row shows corresponding simulation results. Responses are shown for different combinations of stimuli under different attentional conditions. (a) Effects of spatial attention to the preferred stimulus in a pair of stimuli. Neurophysiological data showing the response of a single neuron in V2 (adapted from Reynolds et al., 1999). (b) Effects of spatial attention to the non-preferred stimulus in a pair of stimuli. Neurophysiological data showing the averaged response for a population of cells in V4 (adapted from Reynolds and Desimone, 2003). (c) Effects of featural attention for a pair of stimuli. Neurophysiological data showing the averaged response for a population of cells in V4 (adapted from Chelazzi et al., 2001).

PC/BC model using orientation tuning rather than direction of motion tuning (see Fig. 14c).

For neurons in the ventral pathway the response to the preferred stimulus is reduced by the introduction of a second, non-preferred, stimulus within the RF (Reynolds et al., 1999; Zoccolan et al., 2005). Hence, rather than being processed independently, multiple stimuli within the same RF appear to compete in a mutually suppressive manner (Kastner and Ungerleider, 2000). Attention to the preferred stimulus in the pair increases the recorded response, so that it is more similar to the response that is generated by the preferred stimulus when presented in isolation (see Fig. 15a). In contrast, attention to the non-preferred stimulus in the pair decreases the recorded response, so that it is more similar to the response that is generated by the non-preferred stimulus when presented in isolation (see Fig. 15b). Similar results have been demonstrated for cells in cortical areas V2, V4, inferior temporal cortex, in area MT of the dorsal pathway, and in prefrontal cortex (Everling et al., 2002; Luck et al., 1997; Moran and Desimone, 1985; Reynolds et al., 1999; Reynolds and Desimone, 1999, 2003). The PC/BC model produces a similar pattern of results, as shown in Fig. 15a and b.

The results discussed above show that for spatial attention the response to a pair of stimuli becomes more similar to the response that would be generated if the attended stimulus was presented in isolation. Similar results have been found for selective featural attention (Chelazzi et al., 2001). In this experiment, a stimulus array containing one or two objects was presented. One object in this array may have previously been cued as the target for a saccade. Responses were measured from cells in area V4 with RFs sufficiently large to encompass the stimulus array. Different responses were generated when the target object was the preferred stimulus of the recorded cell compared to when the target was a non-optimal stimulus (see Figure 15c). Equivalent results are generated by the PC/BC model (see Figure 15c).

The experiments above have used the PC/BC model of V1 as a surrogate for simulating attention experiments in other cortical regions such as V2, V4, and MT. One problem of this approach is that the RFs in V1 are small. It is therefore not possible to place multiple stimuli within the cRF and still be able to have those stimuli be the

targets of distinct sources of spatial attention. As can be seen from the results presented in Fig. 15, the poor stimulus does not evoke a response from the recorded neuron when presented in isolation. It is therefore in the ncRF rather than the cRF. Sundberg et al. (2009) performed experiments exploring the effects of spatial attention when stimuli were presented within the cRF and within the suppressive surround of V4 neurons. These effects are very similar to those described above for two stimuli presented within the cRF. Specifically, Sundberg et al. (2009) found that attention to the stimulus in the cRF reduced the suppression caused by a stimulus in the surround whereas attention to the stimulus in the surround increased suppression of the response to the stimulus in the cRF. Hence, the results of the model are also in agreement with this neurophysiological data.

4 Discussion

In many neural network models, including earlier incarnations of the PC/BC model (De Meyer and Spratling, 2009; Spratling, 2008a), synaptic inputs that have modulatory influences have been simulated using different mechanisms, or integrated separately, to those used to implement driving connections (*e.g.*, Balkenius, 1995; Fukushima, 1987; Kay and Phillips, 1997; Lee and Maunsell, 2009; Phillips et al., 1995; Pouget and Sejnowski, 1997; Reynolds and Heeger, 2009; Salinas, 2004; Salinas and Abbott, 1995, 1997; Siegel et al., 2000; Spratling and Johnson, 2004, 2006). In contrast, the version of PC/BC described here, in common with other previous models, treats all synaptic inputs equally and certain inputs generate modulatory influences due to nonlinear dependencies between inputs and outputs (Abbott and Chance, 2005; Brozović et al., 2008; Keith and Crawford, 2008; Murphy and Miller, 2003; Salinas and Abbott, 1996, 2001; Smith and Crawford, 2005; White and Snyder, 2004; Xing and Andersen, 2000; Zipser and Andersen, 1988). The current work goes beyond these previous models in successfully simulating a much larger array of neurophysiological data. In addition, the current model proposes that all pathways, whether bottom-up, lateral, or top-down, can contain both driving and modulatory connections. This is in contrast to the great majority of previous theories of cortical function which propose distinct functional roles for cortical feedforward and feedback pathways (Barlow, 1994; Crick and Koch, 1998; Friston, 2005, 2009; Friston and Büchel, 2000; Hupé et al., 1998; Koch and Segev, 2000; Koerner et al., 1997; Kveraga et al., 2007; Lamme et al., 1998; Mumford, 1992; Olshausen et al., 1993; Rao and Ballard, 1999; Reynolds et al., 1999; Reynolds and Desimone, 1999; Sherman and Guillery, 1998; Spratling, 2002)[1]. However, unlike these previous theories the current model is consistent with recent neurophysiological results showing that cortical feedforward and feedback connections contain both driving and modulatory synapses (Covic and Sherman, 2011; Pasquale and Sherman, 2011). While the model proposes that all cortical pathways can generate both driving and modulatory influences, individual synapses will be either driving or modulatory and, in the absence of changes in connectivity (*e.g.*, due to learning or development) the influence of any individual synapse will remain stable. The role of an individual synapse might therefore be reflected, at a mechanistic level, by changes in synaptic anatomy or physiology. Hence, the current model is not in conflict with extensive data showing that different classes of excitatory synaptic connection have different influences on their post-synaptic targets.

Brain imaging data has shown increased activity in primary visual cortex, in the absence of a visual stimulus, when subjects are performing tasks such as sustained attention or visual imagery (Jack et al., 2006; Kastner et al., 1999; Kosslyn et al., 1999; Muckli, 2010; Munneke et al., 2008; Ress et al., 2000; Silver et al., 2007; Smith and Muckli, 2010). In contrast, such increases in V1 activity have not been so readily observed using single-cell electrophysiology (Luck et al., 1997; McAdams and Maunsell, 1999b; Mehta et al., 2000a; Thiele et al., 2009). The current model is consistent with both sets of results. If we imagine that in Fig. 5b the top-most input is a cortical feedback connection, while the second input is sensory-driven, then the left-hand sub-figure illustrates top-down activity in the absence of visual input. Each individual prediction neuron has a very weak response that might be difficult detect. However, the summed response of the population as a whole is as strong as the summed response generated by the sensory input when presented in isolation (middle sub-figure of Fig. 5b). This diffuse, top-down, excitation might therefore be more readily detected by techniques that measure the activity of large populations of neurons. The current model suggests that connections with greater fan-out will have more modulatory influences. It is difficult to envision how divergent connections produce enhanced activity in a specific sub-set of neurons, rather than more widespread modulation of the large population of neurons to which they connect. However, PC/BC model allows diffuse connections to have very targeted effects, as illustrated on the

[1]Note that if cortical feedback connections were more diffuse than feedforward connections (Salin and Bullier, 1995; Zeki and Shipp, 1988), then the current model would predict that top-down influences would (on average) be more modulatory than bottom-up influences, which would allow the current model to be partially reconciled with some previous theories that propose an asymmetry between feedforward driving influences and feedback modulatory influences (Crick and Koch, 1998; Kveraga et al., 2007; Lamme et al., 1998). The model can also be partially reconciled with some previous models that proposes that cortical feedback connections are suppressive (Barlow, 1994; Mumford, 1992; Rao and Ballard, 1999), as PC/BC proposes that functionally equivalent suppressive operations occur within each cortical region rather than between cortical regions (Spratling, 2008b).

right of Fig. 5b. When a neuron represents the most likely explanation for the current pattern of inputs, its activity can be significantly enhanced by modulatory inputs, while other neurons connected to the same modulatory input receive no excitation: the modulatory excitation effectively becomes routed towards specific neurons and away from others.

The current model suggests that both drivers and modulators arise (in bottom-up, lateral and top-down pathways) as the product of a single computational goal. Previous work has suggested that the computational goal of modulatory influences is to perform coordinate transformations (Salinas and Abbott, 2001; Salinas and Sejnowski, 2001; Salinas and Thier, 2000) or to coordinate learning between functionally specialised local circuits (Kay and Phillips, 2011; Phillips et al., 1995; Phillips and Singer, 1997). Here the proposal is that both drivers and modulators result from the cortex performing perceptual inference. In the PC/BC model, prediction neurons represent hypotheses about the causes underlying the inputs. These predictions are continuously updated to find those that best explain the inputs (in terms of minimising the reconstruction error). Some inputs (either individually or in combination with other inputs) are highly predictive of certain hypotheses, and these therefore have a driving effect on the activation of the prediction neurons that represent those hypotheses. Other inputs are more ambiguous, in that they are consistent with many alternative hypotheses. Such inputs cause little response when presented in isolation, as the evidence they provide is distributed among many alternative hypotheses. However, when such inputs are presented simultaneously with driving inputs they have a modulatory effect on prediction neuron responses. This effect is facilitatory, adding to driving inputs. Suppressive modulatory effects can also occur when prediction neurons representing alternative hypotheses become better explanations of the inputs. In such cases the more likely hypothesis can explain away the evidence (Kersten et al., 2004; Lochmann and Deneve, 2011), suppressing the responses of prediction neurons representing competing hypotheses.

The PC/BC model demonstrates that synaptic connections capable of driving neural responses, and connections that have a modulatory influence on neural activity, can both be explained by the cortex performing perceptual inference. Perceptual inference is a very general computational principle that could underlie many aspects of cognition, and hence, underlie the neural response properties of many cortical areas. Here, it has been shown that a single implementation of this principle can account for a wide range of phenomena including surround suppression, contour integration, gain modulation, spatio-temporal prediction and attention. This has been achieved by modelling the driving and modulatory influences of inputs to a single cortical region in isolation. However, PC/BC processing stages can easily be connected together to create larger models of interacting cortical regions. Simulations of such systems will be the subject of future work with this model.

Acknowledgements

I am grateful to Steven Dakin for kindly providing the code used for generating the contour integration stimuli used for the experiments reported in Fig. 8, and to Bill Phillips for helpful discussions on an earlier draft of this article.

References

Abbott, L. F. and Chance, F. S. (2005). Drivers and modulators from push-pull and balanced synaptic input. *Prog. Brain Res.*, 149:147–55.

Achler, T. and Amir, E. (2008). Input feedback networks: Classification and inference based on network structure. In Wang, P., Goertzel, B., and Franklin, S., editors, *Artificial General Intelligence*, pages 15–26.

Adelson, E. and Bergen, J. (1985). Spatiotemporal energy models for the perception of motion. *J. Opt. Soc. Am. A Opt. Image Sci. Vis.*, 2:284–99.

Andersen, R. A., Essick, G. K., and Siegel, R. M. (1985). Encoding of spatial location by posterior parietal neurons. *Science*, 230(4724):456–8.

Andersen, R. A. and Mountcastle, V. B. (1983). The influence of the angle of gaze upon the excitability of the light-sensitive neurons of the posterior parietal cortex. *J. Neurosci.*, 3(3):532–48.

Angelucci, A. and Bressloff, P. C. (2006). Contribution of feedforward, lateral and feedback connections to the classical receptive field center and extra-classical receptive field surround of primate V1 neurons. *Prog. Brain Res.*, 154:93–120.

Angelucci, A. and Bullier, J. (2003). Reaching beyond the classical receptive field of V1 neurons: horizontal or feedback axons? *J. Physiol. Paris*, 97(2-3):141–54.

Baker, P. M. and Bair, W. (2012). Inter-neuronal correlation distinguishes mechanisms of direction selectivity in cortical circuit models. *J. Neurosci.*, 32(26):8800–16.

Balkenius, C. (1995). Multi-modal sensing for robot control. In Niklasson, L. F. and Bodén, M. B., editors, *Current trends in connectionism*, pages 203–16. Lawrence Erlbaum, Hillsdale, NJ.

Barlow, H. B. (1994). What is the computational goal of the neocortex? In Koch, C. and Davis, J. L., editors, *Large-Scale Neuronal Theories of the Brain*, chapter 1, pages 1–22. MIT Press, Cambridge, MA.

Barlow, H. B. and Levick, W. R. (1965). The mechanism of directionally selective units in rabbit's retina. *J. Physiol. (Lond.)*, 178(3):477–504.

Ben-Shahar, O. and Zucker, S. W. (2004). Geometrical computations explain projection patterns of long range horizontal connections in visual cortex. *Neural Comput.*, 16(3):445–76.

Braun, J. (1999). On the detection of salient contours. *Spatial Vis.*, 12(2):211–25.

Bremmer, F., Distler, C., and Hoffmann, K. P. (1997). Eye position effects in monkey cortex. II. pursuit- and fixation-related activity in posterior parietal areas LIP and 7a. *J. Neurophysiol.*, 77(2):962–77.

Brotchie, P. R., Andersen, R. A., Snyder, L. H., and Goodman, S. J. (1995). Head position signals used by parietal neurons to encode locations of visual stimuli. *Nature*, 375(6528):232–5.

Brozović, M., Abbott, L. F., and Andersen, R. A. (2008). Mechanism of gain modulation at single neuron and network levels. *J. Comput. Neurosci.*, 25:158–68.

Buffalo, E. A., Fries, P., Landman, R., Liang, H., and Desimone, R. (2010). A backward progression of attentional effects in the ventral stream. *Proceedings of the National Academy of Sciences*, 107(1):361–365.

Chang, S. W. and Snyder, L. H. (2010). Idiosyncratic and systematic aspects of spatial representations in the macaque parietal cortex. *Proc. Natl. Acad. Sci. U.S.A.*, 107:7951–6.

Chelazzi, L., Miller, E. K., Duncan, J., and Desimone, R. (2001). Responses of neurons in macaque area V4 during memory-guided visual search. *Cereb. Cortex*, 11(8):761–72.

Chen, C. C., Kasamatsu, T., Polat, U., and Norcia, A. M. (2001). Contrast response characteristics of long-range lateral interactions in cat striate cortex. *Neuroreport*, 12(4):655–661.

Corbetta, M. and Shulman, G. L. (2002). Control of goal-directed and stimulus-driven attention in the brain. *Nat. Rev. Neurosci.*, 3(3):201–15.

Covic, E. N. and Sherman, S. M. (2011). Synaptic properties of connections between the primary and secondary auditory cortices in mice. *Cereb. Cortex*, 21(11):2425–41.

Craft, E., Schütze, H., Niebur, E., and von der Heydt, R. (2007). A neural model of figure-ground organization. *J. Neurophysiol.*, 97:4310–326.

Crick, F. and Koch, C. (1998). Constraints on cortical and thalamic projections: the no-strong-loops hypothesis. *Nature*, 391:245–50.

Dakin, S. C. and Baruch, N. J. (2009). Context influences contour integration. *J. Vis.*, 9(2):1–13.

Dakin, S. C. and Hess, R. F. (1998). Spatial-frequency tuning of visual contour integration. *J. Opt. Soc. Am. A Opt. Image Sci. Vis.*, 15(6):1486–99.

De Meyer, K. and Spratling, M. W. (2009). A model of non-linear interactions between cortical top-down and horizontal connections explains the attentional gating of collinear facilitation. *Vision Res.*, 49(5):553–68.

De Meyer, K. and Spratling, M. W. (2011). Multiplicative gain modulation arises through unsupervised learning in a predictive coding model of cortical function. *Neural Comput.*, 23(6):1536–67.

De Meyer, K. and Spratling, M. W. (in p). A model of partial reference frame transforms through pooling of gain-modulated responses. *Cereb. Cortex*.

Desimone, R. and Duncan, J. (1995). Neural mechanisms of selective visual attention. *Annu. Rev. Neurosci.*, 18:193–222.

Everling, S., Tinsley, C. J., Gaffan, D., and Duncan, J. (2002). Filtering of neural signals by focused attention in the monkey prefrontal cortex. *Nat. Neurosci.*, 5(7):671–6.

Field, D., Hayes, A., and Hess, R. (1993). Contour integration in the human visual system: evidence for a local 'association' field. *Vision Res.*, 33:173–93.

Fitzpatrick, D. (2000). Seeing beyond the receptive field in primary visual cortex. *Curr. Opin. Neurobiol.*, 10:438–43.

Friston, K. J. (2005). A theory of cortical responses. *Philos. Trans. R. Soc. Lond., B, Biol. Sci.*, 360(1456):815–36.

Friston, K. J. (2009). The free-energy principle: a rough guide to the brain? *Trends Cogn. Sci.*, 13(7):293–301.

Friston, K. J. and Büchel, C. (2000). Attentional modulations of effective connectivity from V2 to V5/MT in humans. *Proc. Natl. Acad. Sci. U.S.A.*, 97(13):7591–6.

Fukushima, K. (1987). Neural network model for selective attention in visual pattern recognition and associative recall. *Applied Optics*, 26(23):4985–92.

Galletti, C., Battaglini, P. P., and Fattori, P. (1995). Eye position influence on the parieto-occipital area PO (V6) of the macaque monkey. *Eur. J. Neurosci.*, 7(12):2486–501.

Geisler, W. S., Perry, J. S., Super, B. J., and Gallogly, D. P. (2001). Edge co-occurrence in natural images predicts contour grouping performance. *Vision Res.*, 41(6):711–24.

Grigorescu, C., Petkov, N., and Westenberg, M. A. (2003). Contour detection based on nonclassical receptive field inhibition. *IEEE Trans. Image Proc.*, 12(7):729–39.

Guo, K., Robertson, R. G., Pulgarin, M., Nevado, A., Panzeri, S., Thiele, A., and Young, M. P. (2007). Spatio-temporal prediction and inference by V1 neurons. *Eur. J. Neurosci.*, 26(4):1045–54.

Hansen, T. and Neumann, H. (2008). A recurrent model of contour integration in primary visual cortex. *J. Vis.*, 8(8).

Hess, R. and Field, D. (1999). Integration of contours: new insight. *Trends Cogn. Sci.*, 3:480–86.

Hess, R., Hayes, A., and Field, D. J. (2003). Contour integration and cortical processing. *J. Physiol. Paris*, 97:105–19.

Huang, W., Jiao, L., Jia, J., and Yu, H. (2009). A neural contextual model for detecting peceptually salient contours. *Pattern Recognit. Let.*, 30:985–93.

Hunt, J., Bosking, W., and Goodhill, G. (2011). Statistical structure of lateral connections in the primary visual cortex. *Neural Systems and Circuits*, 1(1):3.

Hupé, J. M., James, A. C., Payne, B. R., Lomber, S. G., Girard, P., and Bullier, J. (1998). Cortical feedback improves discrimination between figure and background by V1, V2 and V3 neurons. *Nature*, 394(6695):784–7.

Jack, A. I., Shulman, G. L., Snyder, A. Z., McAvoy, M., and Corbetta, M. (2006). Separate modulations of human v1 associated with spatial attention and task structure. *Neuron*, 51(1):135–47.

Jones, H. E., Grieve, K. L., Wang, W., and Sillito, A. M. (2001). Surround suppression in primate V1. *J. Neurophysiol.*, 86:2011–28.

Kanwisher, N. and Wojciulik, E. (2000). Visual attention: insights from brain imaging. *Nat. Rev. Neurosci.*, 1(2):91–100.

Kapadia, M. K., Ito, M., Gilbert, C. D., and Westheimer, G. (1995). Improvement in visual sensitivity by changes in local context: parallel studies in human observers and in V1 of alert monkeys. *Neuron*, 15(4):843–856.

Kapadia, M. K., Westheimer, G., and Gilbert, C. D. (2000). Spatial distribution of contextual interactions in primary visual cortex and in visual perception. *J. Neurophysiol.*, 84:2048–62.

Kastner, S., Pinsk, M. A., De Weerd, P., Desimone, R., and Ungerleider, L. G. (1999). Increased activity in human visual cortex during directed attention in the absence of visual stimulation. *Neuron*, 22(4):751–61.

Kastner, S. and Ungerleider, L. G. (2000). Mechanisms of visual attention in the human cortex. *Annu. Rev. Neurosci.*, 23:315–41.

Kay, J. and Phillips, W. A. (1997). Activation functions, computational goals and learning rules for local processors with contextual guidance. *Neural Comput.*, 9(4):895–910.

Kay, J. W. and Phillips, W. A. (2011). Coherent infomax as a computational goal for neural systems. *Bulletin of Mathematical Biology*, 73:344–72.

Keith, G. P. and Crawford, J. D. (2008). Saccade-related remapping of target representations between topographic maps: a neural network study. *J. Comput. Neurosci.*, 24(2):157–78.

Kersten, D., Mamassian, P., and Yuille, A. (2004). Object perception as Bayesian inference. *Annu. Rev. Psychol.*, 55(1):271–304.

Koch, C. and Segev, I. (2000). The role of single neurons in information processing. *Nat. Neurosci.*, 3(supplement):1171–7.

Koerner, E., Tsujino, H., and Masutani, T. (1997). A cortical-type modular neural network for hypothetical reasoning. *Neural Netw.*, 10(5):791–814.

Kosslyn, S. M., Pascual-Leone, A., Felician, O., Camposano, S., Keenan, J. P., Thompson, W. L., Ganis, G., Sukel, K. E., and Alpert, N. M. (1999). The role of area 17 in visual imagery: Convergent evidence from PET and rTMS. *Science*, 284(5411):167–70.

Kveraga, K., Ghuman, A. S., and Bar, M. (2007). Top-down predictions in the cognitive brain. *Brain and Cognition*, 65:145–68.

Lamme, V. A. F., Supèr, H., and Spekreijse, H. (1998). Feedforward, horizontal, and feedback processing in the visual cortex. *Curr. Opin. Neurobiol.*, 8(4):529–35.

Ledgeway, T., Hess, R. F., and Geisler, W. S. (2005). Grouping local orientation and direction signals to extract spatial contours: empirical tests of 'association field' models of contour integration. *Vision Res.*, 45:2511–22.

Lee, J. and Maunsell, J. H. R. (2009). A normalization model of attentional modulation of single unit responses. *PLoS ONE*, 4(2):e4651.

Li, W. and Gilbert, C. D. (2002). Global contour saliency and local colinear interactions. *J. Neurophysiol.*, 88:2846–56.

Li, Z. (1998). A neural model of contour integration in the primary visual cortex. *Neural Comput.*, 10:903–40.

Lochmann, T. and Deneve, S. (2011). Neural processing as causal inference. *Curr. Opin. Neurobiol.*, 21(5):774–81.

Loffler, G. (2008). Perception of contours and shapes: low and intermediate stage mechanisms. *Vision Res.*,

48(20):2106–27.
Luck, S. J., Chelazzi, L., Hillyard, S. A., and Desimone, R. (1997). Neural mechanisms of spatial selective attention in areas V1, V2, and V4 of macaque visual cortex. *J. Neurophysiol.*, 77:24–42.
Markov, N. T. and Kennedy, H. (2013). The importance of being hierarchical. *Curr. Opin. Neurobiol.*, 23(2):187–94.
Martinez-Trujillo, J. C. and Treue, S. (2004). Feature-based attention increases the selectivity of population responses in primate visual cortex. *Curr. Biol.*, 14:744–51.
McAdams, C. J. and Maunsell, J. H. R. (1999a). Effects of attention on orientation-tuning functions of single neurons in macaque cortical area V4. *J. Neurosci.*, 19(1):431–41.
McAdams, C. J. and Maunsell, J. H. R. (1999b). Effects of attention on the reliability of individual neurons in monkey visual cortex. *Neuron*, 23:765–73.
McAdams, C. J. and Maunsell, J. H. R. (2000). Attention to both space and feature modulates neuronal responses in macaque area V4. *J. Neurophysiol.*, 83(3):1751–5.
Mehta, A. D., Ulbert, I., and Schroeder, C. E. (2000a). Intermodal selective attention in monkeys. I: distribution and timing of effects across visual areas. *Cereb. Cortex*, 10:343–58.
Mehta, A. D., Ulbert, I., and Schroeder, C. E. (2000b). Intermodal selective attention in monkeys. II: physiological mechanisms of modulation. *Cereb. Cortex*, 10:359–70.
Mizobe, K., Polat, U., Pettet, M. W., and Kasamatsu, T. (2001). Facilitation and suppression of single striate-cell activity by spatially discrete pattern stimuli presented beyond the receptive field. *Vis. Neurosci.*, 18(3):377–91.
Moran, J. and Desimone, R. (1985). Selective attention gates visual processing in the extrastriate cortex. *Science*, 229(4715):782–4.
Motter, B. C. (1993). Focal attention produces spatially selective processing in visual cortical areas V1, V2, and V4 in the presence of competing stimuli. *J. Neurophysiol.*, 70(3):909–19.
Muckli, L. (2010). What are we missing here? brain imaging evidence for higher cognitive functions in primary visual cortex V1. *International Journal of Imaging Systems and Technology*, 20(2):131–9.
Muckli, L. and Petro, L. S. (2013). Network interactions: non-geniculate input to V1. *Curr. Opin. Neurobiol.*, 23(2):195–201.
Mumford, D. (1992). On the computational architecture of the neocortex II: the role of cortico-cortical loops. *Biol. Cybern.*, 66:241–51.
Mundhenk, T. N. and Itti, L. (2005). Computational modeling and exploration of contour integration for visual saliency. *Biol. Cybern.*, 93:188–212.
Munneke, J., Heslenfeld, D. J., and Theeuwes, J. (2008). Directing attention to a location in space results in retinotopic activation in primary visual cortex. *Brain Res.*, 1222:184–91.
Murphy, B. K. and Miller, K. D. (2003). Multiplicative gain changes are induced by excitation or inhibition alone. *J. Neurosci.*, 23:10040–51.
Olshausen, B. A., Anderson, C. H., and Van Essen, D. C. (1993). A neurobiological model of visual attention and invariant pattern recognition based on dynamic routing of information. *J. Neurosci.*, 13(11):4700–19.
Parent, P. and Zucker, S. (1989). Trace inference, curvature consistency, and curve detection. *IEEE Trans. Pattern Anal. Mach. Intell.*, 11(8):823–39.
Pasquale, R. D. and Sherman, S. M. (2011). Synaptic properties of corticocortical connections between the primary and secondary visual cortical areas in the mouse. *J. Neurosci.*, 31(46):16494–506.
Pettet, M. W. (1999). Shape and contour detection. *Vision Res.*, 39(3):551–7.
Phillips, W. A., Kay, J., and Smyth, D. (1995). The discovery of structure by multi-stream networks of local processors with contextual guidance. *Network*, 6(2):225–46.
Phillips, W. A. and Singer, W. (1997). In search of common foundations for cortical computation. *Behav. Brain Sci.*, 20(4):657–722.
Polat, U., Mizobe, K., Pettet, M. W., Kasamatsu, T., and Norcia, A. M. (1998). Collinear stimuli regulate visual responses depending on cells contrast threshold. *Nature*, 391(6667):580–4.
Pollen, D. A. (1999). On the neural correlates of visual perception. *Cereb. Cortex*, 9(1):4–19.
Pouget, A. and Sejnowski, T. J. (1997). Spatial transformations in the parietal cortex using basis functions. *J. Cogn. Neurosci.*, 9(2):222–37.
Rao, R. P. N. and Ballard, D. H. (1999). Predictive coding in the visual cortex: a functional interpretation of some extra-classical receptive-field effects. *Nat. Neurosci.*, 2(1):79–87.
Rao, R. P. N. and Sejnowski, T. J. (1999). Predictive sequence learnng in recurrent neocortical circuits. In *Advs. Neural Info. Proc. Sys.*
Reggia, J. A. (1985). Virtual lateral inhibition in parallel activation models of associative memory. In *Proc. Int. Joint Conf. on Artif. Intell.*, volume 1, pages 244–8.
Reichardt, W. (1961). Autocorrelation, a principle for the evaluation of sensory information by the central nervous

system. In Rosenblith, W. A., editor, *Sensory Communication*, pages 303–17. Massachusetts Institutes of Technology, Cambridge, MA.

Ress, D., Backus, B. T., and Heeger, D. J. (2000). Activity in primary visual cortex predicts performance in a visual detection task. *Nat. Neurosci.*, 3(9):940–5.

Reynolds, J. H., Chelazzi, L., and Desimone, R. (1999). Competitive mechanisms subserve attention in macaque areas V2 and V4. *J. Neurosci.*, 19:1736–53.

Reynolds, J. H. and Desimone, R. (1999). The role of neural mechanisms of attention in solving the binding problem. *Neuron*, 24(1):19–29.

Reynolds, J. H. and Desimone, R. (2003). Interacting roles of attention and visual salience in V4. *Neuron*, 37:853–63.

Reynolds, J. H. and Heeger, D. J. (2009). The normalization model of attention. *Neuron*, 61(2):168–85.

Salin, P. A. and Bullier, J. (1995). Corticocortical connections in the visual system: structure and function. *Physiol. Rev.*, 75:107–54.

Salinas, E. (2004). Fast remapping of sensory stimuli onto motor actions on the basis of contextual modulation. *J. Neurosci.*, 24(5):1113–8.

Salinas, E. and Abbott, L. F. (1995). Transfer of coded information from sensory to motor networks. *J. Neurosci.*, 15:6461–74.

Salinas, E. and Abbott, L. F. (1996). A model of multiplicative neural responses in parietal cortex. *Proc. Natl. Acad. Sci. U.S.A.*, 93:11956–61.

Salinas, E. and Abbott, L. F. (1997). Attentional gain modulation as a basis for translation invariance. In Bower, J., editor, *Computational Neuroscience: Trends in Research*. Plenum Press, New York, NY.

Salinas, E. and Abbott, L. F. (2001). Coordinate transformations in the visual system: how to generate gain fields and what to compute with them. *Prog. Brain Res.*, 130:175–90.

Salinas, E. and Sejnowski, T. J. (2001). Gain modulation in the central nervous system: where behavior, neurophysiology and computation meet. *The Neuroscientist*, 7(5):430–40.

Salinas, E. and Thier, P. (2000). Gain modulation: a major computational principle of the central nervous system. *Neuron*, 27:15–21.

Schroeder, C. E., Mehta, A. D., and Foxe, J. J. (2001). Determinants and mechanisms of attentional modulation of neural processing. *Frontiers in Bioscience*, 6:d672–84.

Seriès, P., Lorenceau, J., and Frégnac, Y. (2003). The 'silent' surround of V1 receptive fields: theory and experiments. *J. Physiol. Paris*, 97(4-6):453–74.

Sherman, S. M. and Guillery, R. W. (1998). On the actions that one nerve cell can have on another: distinguishing "drivers" from "modulators". *Proc. Natl. Acad. Sci. U.S.A.*, 95:7121–6.

Shipp, S. (2004). The brain circuitry of attention. *Trends Cogn. Sci.*, 8(5):223–30.

Siegel, M., Körding, K. P., and König, P. (2000). Integrating top-down and bottom-up sensory processing by somato-dendritic interactions. *J. Comput. Neurosci.*, 8:161–73.

Sigman, M., Cecchi, G. A., Gilbert, C. D., and Magnasco, M. O. (2001). On a common circle: natural scenes and gestalt rules. *Proc. Natl. Acad. Sci. U.S.A.*, 98(4):1935–40.

Silver, M. A., Ress, D., and Heeger, D. (2007). Neural correlates of sustained spatial attention in human early visual cortex. *J. Neurophysiol.*, pages 229–37.

Smith, F. W. and Muckli, L. (2010). Nonstimulated early visual areas carry information about surrounding context. *Proc. Natl. Acad. Sci. U.S.A.*, 107(46):20099–103.

Smith, M. and Crawford, J. (2005). Distributed population mechanism for the 3-D oculomotor reference frame transformation. *J. Neurophysiol.*, 93:1742–61.

Spratling, M. W. (2002). Cortical region interactions and the functional role of apical dendrites. *Behav. Cogn. Neurosci. Rev.*, 1(3):219–28.

Spratling, M. W. (2008a). Predictive coding as a model of biased competition in visual selective attention. *Vision Res.*, 48(12):1391–408.

Spratling, M. W. (2008b). Reconciling predictive coding and biased competition models of cortical function. *Front. Comput. Neurosci.*, 2(4):1–8.

Spratling, M. W. (2010). Predictive coding as a model of response properties in cortical area V1. *J. Neurosci.*, 30(9):3531–43.

Spratling, M. W. (2011). A single functional model accounts for the distinct properties of suppression in cortical area V1. *Vision Res.*, 51(6):563–76.

Spratling, M. W. (2012a). Predictive coding accounts for V1 response properties recorded using reverse correlation. *Biol. Cybern.*, 106(1):37–49.

Spratling, M. W. (2012b). Unsupervised learning of generative and discriminative weights encoding elementary image components in a predictive coding model of cortical function. *Neural Comput.*, 24(1):60–103.

Spratling, M. W. (2013). Image segmentation using a sparse coding model of cortical area V1. *IEEE Trans. Image Proc.*, 22(4):1631–43.

Spratling, M. W. and Johnson, M. H. (2004). A feedback model of visual attention. *J. Cogn. Neurosci.*, 16(2):219–37.

Spratling, M. W. and Johnson, M. H. (2006). A feedback model of perceptual learning and categorisation. *Vis. Cogn.*, 13(2):129–65.

Sundberg, K. A., Mitchell, J. F., and Reynolds, J. H. (2009). Spatial attention modulates center-surround interactions in macaque visual area V4. *Neuron*, 61:1–12.

Their, P., Haarmeier, T., and Ignashchenkova, A. (2002). The functional architecture of attention. *Curr. Biol.*, 12(5):R158–R162.

Thiele, A., Pooresmaeili, A., Delicato, L. S., Herrero, J. L., and Roelfsema, P. R. (2009). Additive effects of attention and stimulus contrast in primary visual cortex. *Cereb. Cortex*, 19:2970–81.

Treue, S. (2001). Neural correlates of attention in primate visual cortex. *Trends Neurosci.*, 24(5):295–300.

Treue, S. and Martinez-Trujillo, J. C. (1999). Feature-based attention influences motion processing gain in macaque visual cortex. *Nature*, 399(6736):575–9.

Ursino, M. and La Cara, G. E. (2004). A model of contextual interactions and contour detection in primary visual cortex. *Neural Netw.*, 17(5–6):719–35.

Vecera, S. P. and O'Reilly, R. C. (1998). Figure-ground organization and object recognition processes: An interactive account. *J. of Expt. Psyc.: Human Percept. & Perform.*, 24:441–62.

Vonikakis, V., Gasteratos, A., and Andreadis, I. (2006). Enhancement of perceptually salient contours using a parallel artificial cortical network. *Biol. Cybern.*, 94(3):192–214.

Watt, R., Ledgeway, T., and Dakin, S. C. (2008). Families of models for gabor paths demonstrate the importance of spatial adjacency. *J. Vis.*, 8(7):1–19.

White, R. L. and Snyder, L. H. (2004). A neural network model of flexible spatial updating. *J. Neurophysiol.*, 91(4):1608–19.

Xing, J. and Andersen, R. A. (2000). Models of the posterior parietal cortex which perform multimodal integration and represent space in several coordinate frames. *J. Cogn. Neurosci.*, 12(4):601–14.

Yen, S. and Finkel, L. (1998). Extraction of perceptually salient contours by striate cortical networks. *Vision Res.*, 38(5):719–41.

Young, R. A. and Lesperance, R. M. (2001). The gaussian derivative model for spatial-temporal vision: II cortical data. *Spatial Vis.*, 14:321–89.

Zeki, S. and Shipp, S. (1988). The functional logic of cortical connections. *Nature*, 335:311–7.

Zhaoping, L. (2005). Border ownership from intracortical interactions in visual area V2. *Neuron*, 47:143–53.

Zipser, D. and Andersen, R. A. (1988). A back-propagation programmed network that simulates response properties of a subset of posterior parietal neurons. *Nature*, 331(6158):679–84.

Zoccolan, D., Cox, D. D., and DiCarlo, J. J. (2005). Multiple object response normalization in monkey inferotemporal cortex. *J. Neurosci.*, 25(36).